LEIDS UNIVERSITAIR MEDISCH CENTRUM

Delft University of Technology

Value-Assessment of Computer-Assisted Navigation Strategies during Percutaneous Needle Placement

Imke Boekestijn

Delft University of Technology

Biomedical Engineering (Medical Physics)

Delft, the Netherlands

Daily Supervisor:

Drs. D.D.D. Rietbergen

Responsible Supervisor:

Prof. Dr. J. Dankelman

Defense Committee:

Dr. N. Bhattacharya
Dr. J.J. van den Dobbelsteen
Prof. Dr. F.W.B. van Leeuwen

June 22, 2021

Abstract

Introduction: In daily practice, at interventional radiology (IR), percutaneous needle placement (e.g. biopsy and ablation) is generally performed under real time guidance of morphological imaging (US or CT). However, in some cases obtaining representative specimen can be challenging causing repeated biopsies or shift to open procedures. And so alternatively, needle placement can occur using computer-assisted needle navigation strategies that rely on pre-interventional images such as (PET-) CT scans. To unravel the impact of needle navigation strategies in addition to the use of ultrasound guidance, we recorded and analyzed the needle- and US-movements during exercises performed in a custom abdominal biopsy phantom.

Methods: custom abdominal biopsy phantom was generated using synthetic ballistic gel, bone-like structures, spherical targets and fiducials for both electromagnetic (EM) and optical tracking. Following administration of a mixture containing ^{18}F-FDG and $^{99m}TcO_4^-$ and prior to the needle interventions, the phantom was subjected to PET-CT and SPECT-CT imaging. After presenting them with the 3D imaging data-sets interventions were performed by both novices and experts (n = 20 in total). The exercise comprised of three consecutive steps: 1) US guided biopsy, 2) US guided PET-CT-navigated biopsy (US + Nav), 3) US guided PET-CT-navigated biopsy + virtual needle guidance (US + Nav + NG). Each step was performed on a different target and the exercise continued until the participant was successful. In all cases, we recorded the traveled paths determined in 3D (i.e., x, y, and z) of both the needle and the ultrasound probe. Tracking was realized by using a fiducial-based optical tracking system. Following the visualization of the traveled paths in MATLAB® (the MathWorks, Inc), we used custom software to analyze movement features such as speed, acceleration, jerkiness, straightness index, angular dispersion and curvature and related these dexterity (Dx) scores. We also analyzed missteps such as corrections and retractions and combined these with dexterity features to create decision making (DM) scores.

Results: Analysis of the needle trajectories indicated a decrease of jerkiness for the novices as a result of the additional navigational technologies (US vs Us + Nav + NG; p = 0.033). In this particular group US + Nav influenced both the dexterity and decision making more positively than US + Nav + NG ($Dx_{80(US)}$ = 20.0 (US) vs $Dx_{80(US+Nav)}$ = 5.19 vs $Dx_{80(US+Nav+NG)}$ = 9.73 and $Dm_{80(US)}$ = 12.6 vs $Dm_{80(US+Nav)}$ = 2.78 vs $Dm_{80(US+Nav+NG)}$ = 5.90). For experts, the navigational technologies negatively influenced the dexterity of experts similar but reversed with scores of $Dx_{80(US)}$ = 2.92 vs $Dx_{80(US+Nav)}$ = 12.1 vs $Dx_{80(US+Nav+NG)}$ = 9.33 and negatively influenced their decision making by increasing total pathlength, corrections and retractions (US vs US + Nav; p = 0.035, p = 0.001 and p = 0.006, respectively), thus worsening decision making scores ($Dm_{80(US)}$ = 0.569 vs $Dm_{80(US+Nav)}$ = 7.66 vs $Dm_{80(US+Nav+NG)}$ = 6.38).

Conclusion: By recording and analyzing the movement paths of the ultrasound probe and biopsy needle trajectories it has become possible to make an objective value-assessment on the performance enhancement created by computers-assisted navigation strategies. These preliminary findings suggest that technological refinements have a different impact on novices and experts and that increasing the technological complexity can reduce its impact.

Keywords: Navigation systems, Image-guided biopsy, PET, Computer assistance, Performance assessment

Acknowledgements

First and foremost, I would like to express my gratitude towards my daily supervisor Drs. Daphne D. D. Rietbergen for giving me this opportunity to perform such an interesting study under her supervision. You gave me the room to pursue my ideas and wises and become a more independent researcher while still giving me the best advice and feedback to raise my knowledge and skills. Beside the excellent supervision you were also great company for the weekly coffees and I hope we can continue this partnership over the next couple of years. Furthermore, I would like to thank Prof. Dr. Fijs W. B. van Leeuwen to allow me to do my master research at his group. You are always honest and pushing us to become the best researchers we can be. Due to your help I have extended my knowledge and skills tremendously. I am sure that over the next few years achieve real good science. I also would like to thank Prof. Dr. Ir. Jenny Dankelman for providing supervision from within TU Delft by giving me feedback and new ideas to work with.

Of course my colleagues, and in particular Ir. Samaneh Azargoshasb, Leon J. Slof, Drs. Laurie Pronk and Dr. Ir. Matthias N. van Oosterom, deserve my gratitude as well for helping me with anything and everything, where nothing was too crazy. I sincerely hope we can keep up the good work together with the usual Monday to Friday spirit.

At last, I would like to thank Dr. N. Bhattacharya and Dr. J.J. van den Dobbelsteen for reading my thesis and to be part of my defense committee.

Contents

1. Introduction

Diagnosis of a suspicious lesion is key for the accurate management of patients. In addition to the patient's history, clinical findings, the implications made by different imaging modalities, clinical decision making is very much driven by pathological analysis. For this microscopic analysis of the tissue biology it is of paramount importance to obtain a specimen of the suspicious lesion, so-called biopsy.

In current day practice, biopsy as well as needle-based ablation procedures are guided in real time by ultrasound (US) or computed tomography (CT). Although effective in the majority of lesions, these morphological imaging modalities are, not able to provide information on (diseased) tissues on a molecular level. In the clinic, nuclear medicine provides the benchmark for non-invasive molecular imaging, a prime example being metabolic positron emission tomography (PET) imaging of oncological lesions using ^{18}F-FDG.[1] The high diagnostic accuracy of PET also holds promise to improve the biopsy of lesions active without distinctive morphology and/or contain a high degree of heterogeneity.[2,3]

Minimally invasive (image guided) percutaneous needle biopsy is increasingly being favored over open excisional biopsy; It decreases the patient burden and can increase procedural precision[4-7]. As a consequence many technological advances e.g. hand-held trajectory guidance tools, electronic needle visualization and image fusion[8] have been pursued to guide needle placement in difficult-to-reach lesions e.g. within the liver of patients. In such complex indications, however, the technical skills of the (interventional) radiologist can become limiting. It is for that reason that computer-assisted navigation strategies help to connect interventional ultrasound with e.g. pre-interventional 3D imaging datasets. This connection is facilitated by electromagnetic (EM) or optical tracking systems that track the position of the needle in space[9] and can even virtually present the expected needle path[10]. These concepts are very much in analogy to the use of GPS-based navigation devices that we use in our daily lives. While geography navigation provides an efficient means to travel from A to B, navigation in patients is complicated by the anatomical complexity and tissue motility. There is reported evidence that navigation can advance the decision making process and can improve dexterity[11], but some may consider such technologies as costly and over engineered devices that have little value for expert radiologists.

To unravel the role that computer-assisted needle navigation strategies play in the decision making processes and to quantify the impact of these modalities on dexterity, we studied their use during a needle guidance procedure on an abdominal biopsy phantom. This exercise entailed three steps that were guided by pre-intervention PET-CT data: 1) US-guided biopsy , 2) US-guided PET-CT-navigated biopsy (US + Nav guided), 3) US-guided PET-CT-navigated biopsy + virtual needle guidance (US + Nav + NG guided) (see Figure 1). Using a fiducial-based optical tracking system, we recorded the traveled paths determined in 3D (i.e., x, y, and z) of both the needle and the ultrasound probe and analyzed these movement features. By performing these exercises with both expert (interventional) radiologists and novices, we were not only able to isolate which of the movement components directly impacted dexterity and decision making and relate this impact to experience, but we were also able to define a measure to score procedural dexterity and decision making.

2. Methods

2.1 Phantom Development

To study the dexterity of the performance during a biopsy procedure, a customized abdominal phantom was developed. A more detailed description of the phantom design, preparation and reusing protocol can be found in Appendix A. The phantom was compatible with US, CT, PET and SPECT imaging. The phantom was made out of 10% Ballistic Gelatin (Clear Ballistics, Greenville, SC, USA)), which in turn contained 3D printed structures that mimicked the spine and several ribs (Rigid Resin 4000, Formlabs, Somerville, MA, USA) and included 10 3D-printed spherical lesions (Elastic resin, Formlabs, Somerville, MA, USA) filled with a mixture of Sodium Polyacrylate: 432784-250g (Sigma-Aldrich, Saint Louis, MO, USA) and Glycerol >99.0%: G5516-100ML (Sigma-Aldrich, Saint Louis, MO, USA; diameters of 1.0, 1.5 or 2.0 cm). The phantom was enclosed between two plexiglass plates. The top of one of the plexiglass plates contained a platform to which both an EM active tracker and an optical fiducial were fixated.

To allow for the generation of preoperative PET/CT and SPECT/CT scans of the phantom, five to seven lesions in the phantom were injected with a mixture of both ^{18}F-FDG (10 MBq in total) and $^{99m}TcO_4^-$ diluted in saline (30 MBq in total). These quantities helped to create a realistic SUV value between 1-5 SUV within the lesions[12,13]. After the injection of activity, first a PET-CT was acquired using a Philips Vereos PET/CT-scanner (Philips Medical Systems, Cleveland, OH, USA) with a 288 x 288 matrix and 2 mm slice thickness for the PET, along with a low-dose CT using a 512 x 512 mm and 1 mm slice thickness for attenuation correction. Subsequently, a SPECT-CT was acquired using a Symbia T6 SPECT/CT-scanner (Siemens Medical Solutions, Malvern, PA, USA) wherein the events captured during the SPECT scan were stored in a matrix of 128 x 128 with a slice thickness of 4.8 mm, along with a low-dose CT using a matrix of 512 x 512 and slice thickness of 1.3mm. Images were analyzed using PACS IDS7 (Sectra AB, Linköping, Sweden).

2.2 Navigation Devices and Tracking Systems

The EM tracking system VirtuTRAX (Civco, Kalona, IA) is fully compatible with the LOGIQ™ E10 Ultrasound (GE Healthcare, Milwaukee, WI) and helped facilitate registration between the scan and the phantom.[14] The correlation between the EM tracking sensor within the US probe and the fixated active tracker, allowed co-registration of the real-time US and preprocedural PET-CT. Subsequently, the tracking sensor enclosed within the tip of the needle enabled its navigation towards the target. During the intervention the US images were recorded using a screen recorder (Blackmagic Video Assist 7" 3G), for video analysis. Possible misregistration was reduced during the navigated biopsies through manually correlating anatomical landmarks.

The inability to read out raw coordinate data from the VirtuTRAX tracking system, meant a second (optical) tracking system, Declipse®SPECT (SurgicEye GmbH, Munich, Germany)[15], was required to record the movement paths (or rather coordinate systems) of the needle (after identification of the target) and the US probe (during the entire procedure).[16] To allow this, customized optical fiducials (see Appendix B.3) were placed on both tools. Movement trajectories were analyzed using MATLAB® (the MathWorks, Inc).

2.3 Performance Study Design

In this study the participants (n=20) were categorized in two groups, experts (n=9) and novices (n=11). A participant was considered to be an expert when he or she acquired at least two years of US experience or had clinically applied US-guided needle insertion. For the novice group, participants with

different kinds of background were included, e.g. medicine practitioners without US experience, scientists and engineers.

In the study, target lesions within the phantom were approached with a 17GA biopsy needle. The complete setup is schematically depicted in Figure 1. All participants were asked to perform three different assignments: 1) US guided biopsy, 2) US + Nav guided biopsy, 3) US + Nav + NG guided biopsy. This study set-up explicitly focused on the technological aspects of the procedure. By performing the exercised in one go, we tried to prevent a possible learning curve from influencing the procedure. The study participants were designated a target sphere in the preprocedural PET-CT images which had to be localized with the US probe and directly after, biopsied. In case the target was not biopsied in the first attempt, corrections, retractions and reinsertion of the needle were allowed until the participant was successful. To avoid biases in the study, the approachable targets were randomly distributed throughout the phantom and each assignment was performed on a different target. The instruction sheet given to the participants can be found in Appendix C. Instruction Sheet.

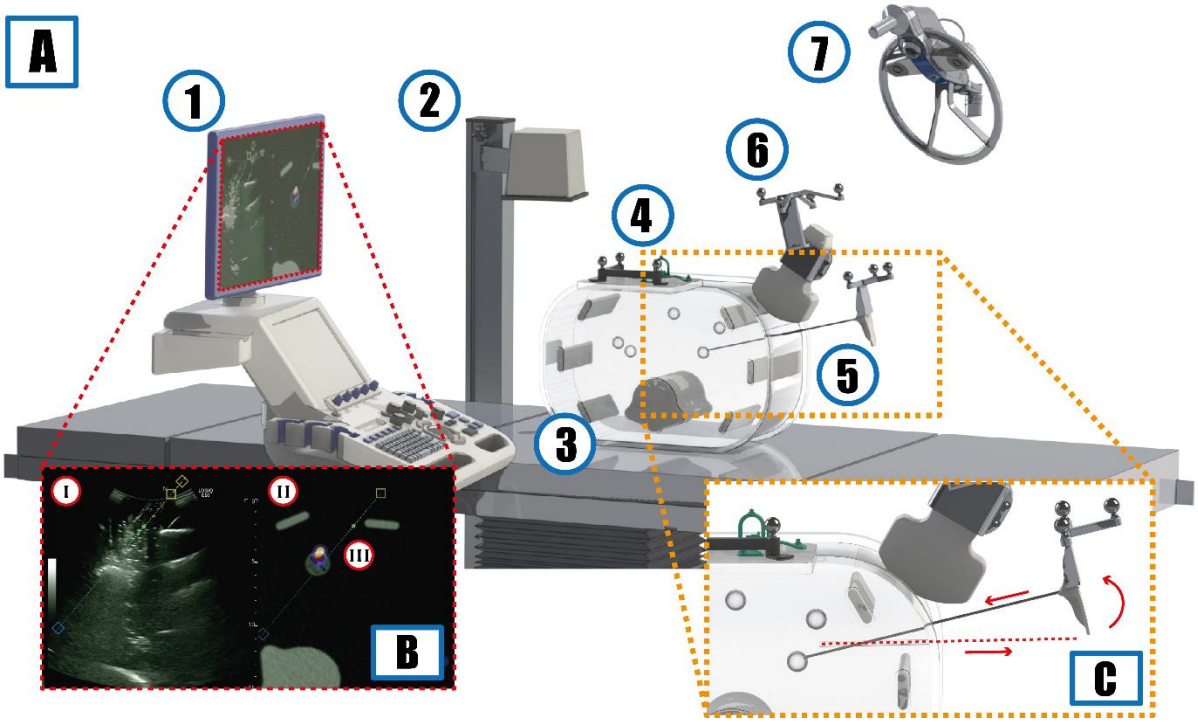

Figure 1. A) The phantom based experimental set up used to study the impact of the additional computer-assisted navigation technology during an image-guided biopsy depicted schematically. (1) The ultrasound (BI) including preprocedural PET-CT navigation (BII) and virtual needle guidance (BIII) , (2) EM transducer, (3) phantom including imitation lesions, (4) EM active tracker and fiducial tracker, (5) biopsy needle with fiducials, (6) US probe including fiducials and (7) Optical near infrared camera. C) shows the retraction and reinsertion movements which can occur during the procedure.

2.4 Data Analysis

The obtained trajectories were quantified through using a custom tortuosity analysis in MATLAB® (the MathWorks, Inc) while a video analysis is performed on the recorded US. The performance metrics adopted in this study (shown in Table 1) includes ultrasound probe and needle handling. Furthermore, the personal experience of the participants are documented through an experience questionnaire which can be found in Appendix D. Experience Questionnaire.

Trajectory analysis

After preprocessing the coordinate data, the 3D paths traveled by the US probe and needle over time were reconstructed in MATLAB® (the MathWorks, Inc). Preprocessing consisted of "stitching" gaps in the trajectory when the instrument was out of the field of view of the tracking camera. The procedure in subdivided in different aspects; wherein the general aspects were analyzed through total pathlength and completion time, dexterity was analyzed according to the temporal features such as speed, acceleration and jerkiness, the fluency of the procedure was based on the straightness index dispersion and curvature of both instruments[17-19]. The decision making process was quantified by extracting the number of corrections and retractions, appearing within the needle trajectory. A correction or retraction was characterized as a direction change in the z-direction; a correction required a directional change with a distance between 10-50 mm and a retraction required a directional change > 50 mm (Figure 1B). Precise calculations methods of the general, dexterity and fluency aspects and the correction and retractions determination can be found in Appendix E. Trajectory analysis.

Dexterity and decision making index

Correlating the different procedural dexterity, fluency and decision making features to the total pathlength normalized over entire data set adopting a min-max normalization, allowed us to define a dexterity and decision making index to score the performance. The dexterity index is calculated considering the total jerkiness in x, y and z-coordinates during the entire procedure from start (t_1) to finish (t_2) and eliminating the effect of amplitude and pathlength with a min-max normalization as shown in Equation 1[20],

$$Dx = \text{norm}\left(\int_{t_1}^{t_2}\left(\frac{\delta^3 x}{\delta t^3}\right)^2 + \left(\frac{\delta^3 y}{\delta t^3}\right)^2 + \left(\frac{\delta^3 z}{\delta t^3}\right)^2 dt\right). \quad (1)$$

The decision making index is dependent on a combination of dexterity features and missteps as well as a successful execution of the exercise. The exercise is successful when the target is punctured, otherwise the decision making score is set on 100, as shown in Equation 2,

$$DM := \begin{cases} wf_1 \cdot J_{extr} + wf_2 \cdot R + wf_3 \cdot C + wf_4 \cdot e^{-\log(ST)}, & target\ punctured \\ 100, & target\ missed. \end{cases} \quad (2)$$

It depends on the number of extremes in jerkiness ($\#J_{extr}$), retractions (R) and corrections (C) and the straightness index (ST). Each of these features are dependent on the total pathlength with their own regression; Appendix F.1, and therefore are all contributing to the decision making with different weight factors. In order to determine the values of these factors, the relation between total pathlength and decision making for each user groups per exercise (US, US + Nav and US + Nav + NG guided biopsy) has to be maximized. This can be achieved by optimizing the sum of all relative R^2 values and using the constraint; $wf_1 + wf_2 + wf_3 + wf_3 = 1$, where wf ranges between [0, 1] with step size 0.02 in MATLAB® (the MathWorks, Inc).

Scoring of US performance

In a well-executed US-guided biopsy it is considered to be of importance that the entire needle is visible within the plane of the US beam throughout the entire procedure.[21] Incorrect placement of the insertion point of the needle or rolling of the US probe hinder good visualization and were therefore considered missteps. Following the ultrasonography performance metrics set by Johnson et al.[22], we

manually quantified the visualization aspects of the procedure on three objectives; 1) determining the percentage in which the target was in field of view (FOV) of the US with respect to the probe usage time, 2) the needle tip was in US's FOV with respect to needle usage time and 3) the entire needle was in plane with respect to time in which the needle tip was in view.

Table 1. Performance metrics to assess the execution of the biopsy procedure.

Procedural Aspect	Feature	Needle	US probe
General	Pathlength s [mm]	x	x
	Completion time t [s]	x	x
Dexterity	Speed v [mm · s^{-1}]	x	x
	Acceleration a [mm · s^{-2}]	x	x
	Jerkiness J [mm · s^{-3}]	x	x
Fluency	Straightness Index ST [-]	x	x
	Angular Dispersion AD [-]	x	x
	Curvature κ [-]	x	x
Decision Making	Corrections ($1 < \Delta z < 50$ mm)	x	-
	Retractions ($\Delta z \geq 50$ mm)	x	-
	Target in View [%]	-	x
	Needle Tip Visualization [%]	-	x
	Total Needle in Plane Visualization [%]	-	x

Statistics

Statistical significance of the features describing procedural dexterity as well as decision making was established via an independent t-test with the SPSS statistical software (IBM SPSS Statistics for Windows, Version 25.0), using a confidence interval of 95%.

3. Results

3.1 Phantom Images

Concerning the gantry imaging, after injection with the radiotracers in five lesions, PET/CT and or SPECT/CT scans could clearly visualize the lesions. On the CT, the 3D printed materials gave specific Hounsfield units of: 368 HU for bone, 138 HU for the lesions and -166 for the ballistic gel. The fused SPECT-CT and PET-CT are shown in Figure 2A and 2B. Typical images acquired with the phantom are shown in Figure 2C On the US images, the lesions present themselves as half spherical thin lines. A small hindrance was caused by the fact that the 3D printed shell of the artificial lesions blocked the signal below the lesion, an effect that did not impact the exercise.

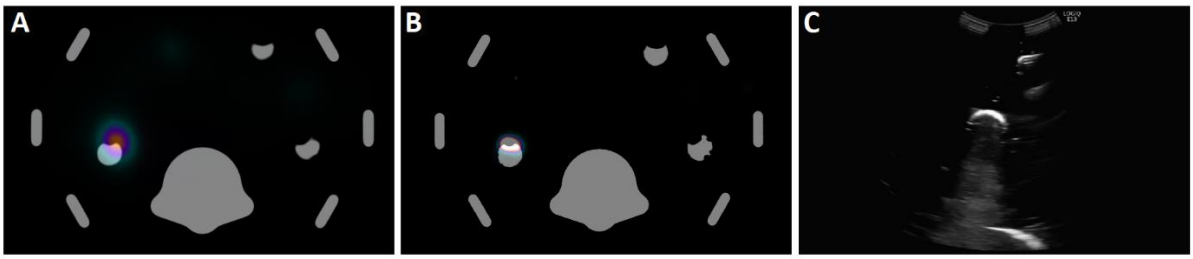

Figure 2. A) Shows an example the acquired SPECT-CT and B) the acquired PET-CT of the phantom with Hounsfield units of: 368 HU for bone, 138 HU for the lesions and -166 for the ballistic gel. C) Shows an example of the customized abdominal phantom on the ultrasonography.

3.2 Performance Study

Analysis of the movement trajectories allowed extraction of unique movement features from individual tasks. Figure 3 shows typical examples of the tracked needle-paths in a 3D Cartesian coordinate of the US guided biopsy, US + Nav guided biopsy, US + Nav + NG guided biopsy of both an expert and a novice. The color gradient of the line matches that of the bar and represent speed of the needle tip. Clearly the trajectories of experts and novices tracks differ during the first exercise (Figure 3Ai vs ii); the expert movements are more focused. This visual assessment was confirmed by t-distributed stochastic neighbor embedding (tSNE) analysis wherein a total of 10 features consisting of the needle based movement features and decision making aspects (Table 1), reduced to 9 with a principal component analysis (PCA), are used as is shown in Figure 3Aiii. The differentiation between novices and experts, vanishes when navigation and virtual needle guidance are included (Figure 3B and 3C respectively). While the movements of novices get more focused, it appears the movements of the experts become more erratic. This suggests that the value of the navigation technologies tested may vary based on the users' experience.

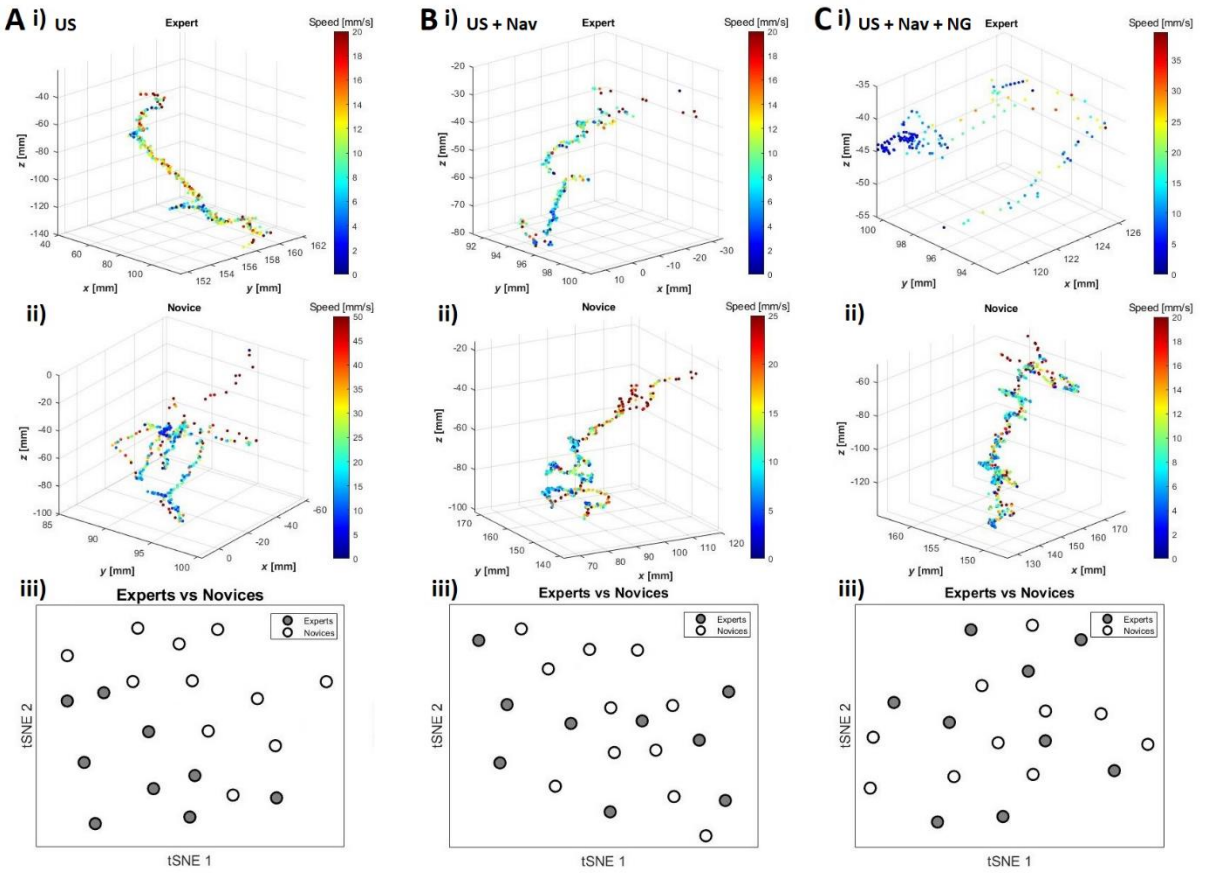

Figure 3. Tracked needle tip paths depicted in a 3D graph 9of all three assignments, US guided (A), US + Nav guided and navigated (B) and US + Nav + NG guided (C) of both an expert (i) and a novice (ii). The color bar indicates the movement speed at each point within the path. iii) Shows the tSNE results of a comparison between experts and novices for each assignment individually, in cooperating 9 features after applying PCA on a total of 10 features.

3.2.1 Correlation between Features for Dexterity and Decision Making

In this study, we were able to extract and quantify movement features (Table 1) from the needle path trajectories to analyze both dexterity, fluency, and decision making features. The in depth results can be found in Appendix F.2; Figures F.2 – F.4. By assuming that lesser and more constant movements would lead to a more accurate executed biopsy procedure, the values are depicted in a scale wherein the lowest signal equals the most optimal performance. Following the analysis of the individual

components, we studied the correlation between dexterity and decision making features. Plotting the velocity and acceleration changes (the amount of peaks in the acceleration and jerkiness respectively) for each individual track against both the corresponding corrections and retractions resulted in a linear correlation between temporal features and the missteps in the decision making as shown in Figure 4. The corrections (Figure 4A) are linearly correlated with the total pathlength, speed and acceleration changes with R^2 values of 0.48, 0.40 and 0.45, respectively. These same features are also strongly correlated with the retractions (Figure 4B) with, R^2 values of 0.89, 0.83 and 0.88, respectively. Combined this suggests that increased procedural performance (less corrections and retractions) occurs in procedures were both velocity and acceleration are more consistent.

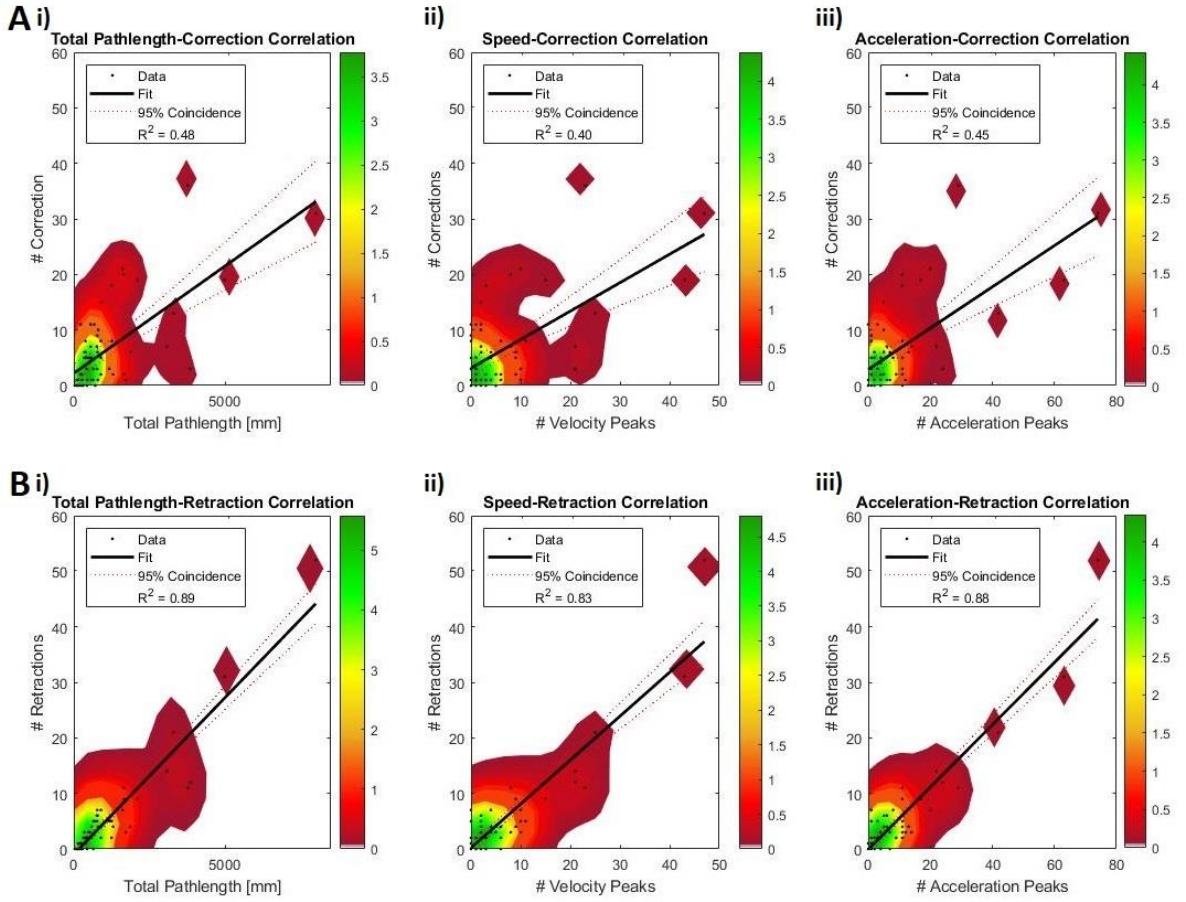

Figure 4. The total pathlength (i), speed (ii) and acceleration (iii) changes of the needle path are linearly correlated with the corrections (A) and retractions (B). The colorbar indicates the density occurrence of corrections and retractions.

3.2.2 Movement Feature Comparison and Dexterity Scores

Extracting quantitative movement features (Table 1) from the movement paths allowed us to score dexterity and fluency and facilitated comparisons between exercises, modalities tracked (needle vs ultrasound) as well as groups (expert vs novice). From this data (Appendix F.2; Figure F.2) a number of significant changes within the needle tracks could be extracted to compare technological strategies as well as user groups. First, a decrease of jerkiness and angular dispersion for novices and experts respectively as a result of virtual needle guidance (US guided vs US + Nav + NG guided; p=0.033 and p=0.027). Second we observed a decrease of the inversed straightness index and angular dispersion when using virtual needle guidance (experts vs novices; p=0.046 and p=0.05 respectively). The most significant changes within the path of the ultrasound probe are mainly found in the experts vs novices comparison; experts show a higher inversed straightness index and angular dispersion compared to novices (p=0.036 and p=0.008, respectively), a lower speed, but a larger jerkiness (p = 0.006 and p =

0.024, respectively) (Appendix F.2; Figure F.3). When looking at overall the median results (Appendix F.2; Figure F.4) it becomes evident that the navigation technologies have little impact on the use of the ultrasound device in either group.

For the needle movements we see that navigation provides more improvements in dexterity; speed, acceleration, jerkiness for novices than experts (Figure 5A). Interestingly, use of navigation make the experts score lower on angular dispersion and curvature. The latter trend within the expert group was corrected when virtual needle guidance was applied. By using the relationship between features presented in Equation 1, we created a valuable measure to compare the impact of technologies linearly with the pathlength; R^2 values for the dexterity score of 0.93, 0.97 and 0.99 for experts (i) and 0.96, 0.84 and 0.99 for novices (ii) for US guided biopsy (red), US + Nav guided biopsy (blue) and US + Nav + NG guided biopsy (green) respectively, as shown in Figure 5B. The score given to each exercise is relies on the 80 % mark, which is based on the proficiency score used in surgical training[23] (in depth information can be found in Appendix F.3). Interestingly, for the expert group the dexterity score was increased with the introduction of navigation (Dx_{80} = 2.92 vs Dx_{80} = 12.1) and is slightly reduced when virtual needle guidance is added to the procedure with scores of Dx_{80} = 12.1 vs Dx_{80} = 9.33. A similar but reversed trend can be found for the novice group, where navigation has a positive influence leading to better dexterity (Dx_{80} = 20.0 vs Dx_{80} = 5.19). And once again virtual needle guidance is reversing this effect; Dx_{80} = 5.19 vs Dx_{80} = 9.73 which is in line with the trend shown in Figure 5A. As expected, using the conventional technique of performing the procedure US guided, the experts score substantially lower on both dexterity and decision making.

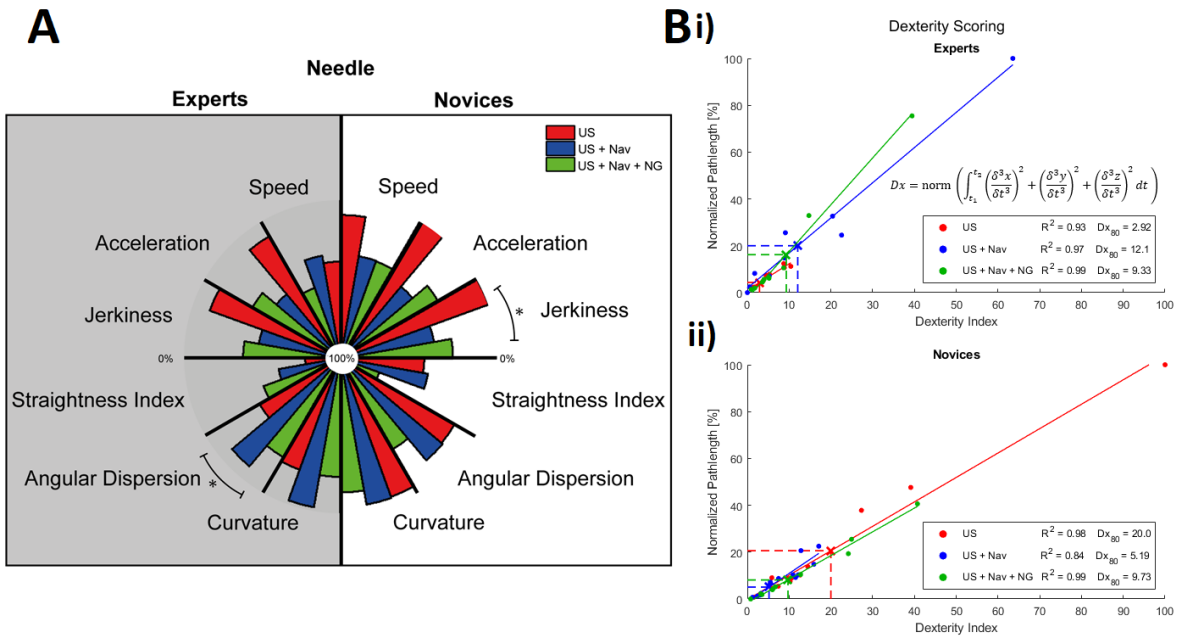

*Figure 5. A) An comparative overview of the dexterity and fluency features of the needle for the additional technology (US guided biopsy (red), US + Nav guided biopsy (blue) and US + Nav + NG guided (green)) for both experts (gray) and novices (white), where * indicates a significance of p<0.05. B) shows the dexterity score given to both experts and novices for each of these technologies.*

3.2.3 Missteps and Decision Making Scores

In an interventional procedure, corrections and retractions, and therefore indirect the pathlength of the needle path can induce tissue damage and so, should be considered as missteps and are correlated to the dexterity as shown in Figure 4. Most importantly, it appears that increasing the technological complexity with navigation negatively impacts the experts performance (see Figure 6A and Appendix

F.4; Figure F.7). This is examplified by an increase in needle pathlength, corrections and retractrions (US guided vs US + Nav guided; p=0.035, p=0.001 and p=0.029 respectively). This could again be corrected using needle guidance. Results are once more different for the novice group, were navigation impacts the decision making positively by significantly reducing the pathlength (US guided vs US + Nav guided; p = 0.016). However, the needle guidance also appears to create some doubt, which converts to a significant increase in corrections (US + Nav guided vs US + Nav + NG guided; p = 0.006). In order to score the users on their decision making, we created a decision making index using a combination of missteps and dexterity as shown in Equation 2. This index allows for linear comparison between the different technologies; US guided biopsy (red), US + Nav + NG guided biopsy (blue) and US + Nav + NG guided biopsy with R^2 values of 0.63, 0.97, 0.95 for experts (i) and 0.94, 0.85 and 0.97 for novices (ii) respectively, as shown in Figure 6B. Surprisingly, the experts decision making score (DM_{80}) decreased when navigation was introduced (DM_{80} = 0.569 vs DM_{80} = 7.66) and which was slightly reversed when adding virtual needle guidance to the procedure (DM_{80} = 7.66 vs DM_{80} = 6.38). For the novice group the reverse trend is visible where navigation positively influenced the decision making; DM_{80} = 12.6 vs DM_{80} = 2.78 and once again the complexity of virtual needle guidance lead to worsen the decision making by enlarging the score; DM_{80} = 2.78 vs DM_{80} = 5.90.

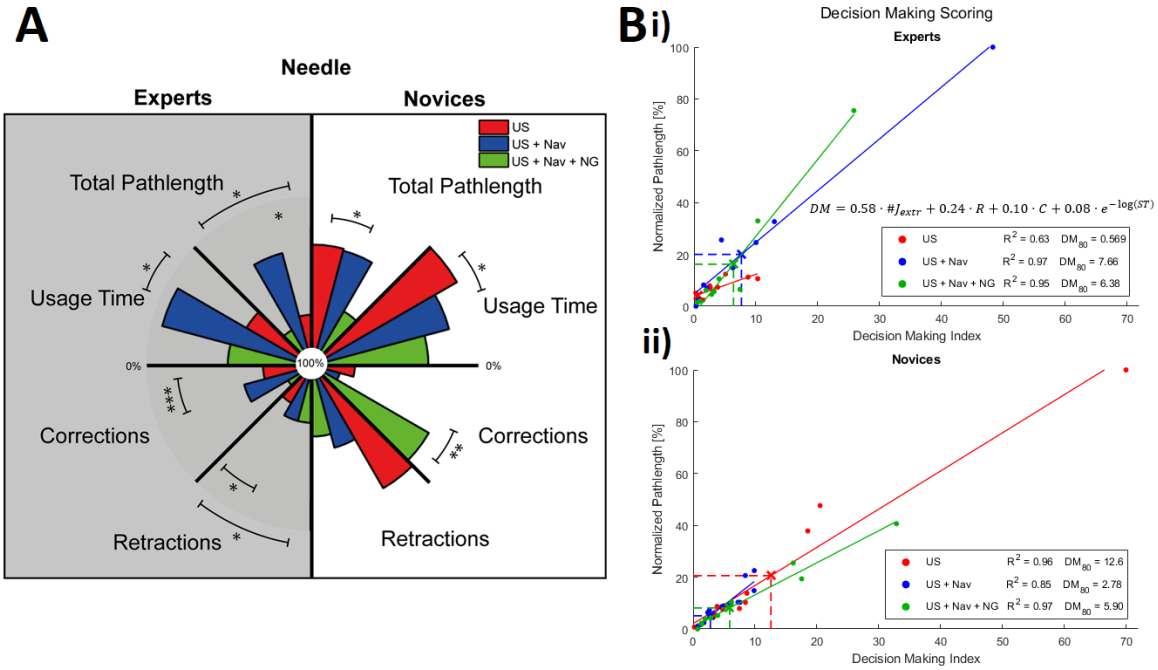

*Figure 6. A) An overview of the general and decision making features to compare the additional technology (US guided biopsy (red), US + Nav guided biopsy (blue) and US + Nav + NG guided (green)) for both experts (gray) and novices (white), where the significance is indicates by *; p<0.05, **; p<0.01 and ***; p<0.001. B) shows the decision making score given to both experts and novices for each of these technologies.*

Video analysis of the US-images allowed for an evaluation of the US-based performance metrics (Appendix F.4; Figure F.8 and Figure F.9, respectively). The additional navigation positively impacted the US-based performances of novices by increasing the total needle in plane percentage (US guided vs US + Nav guided; p=0.004) and even leading to a better visualization compared to experts (experts vs novices; p=0.027). Navigation even leads to a reduction in total pathlength and usage time of the US probe suggesting a positive influence on the biopsy site localization process. However, the positive influence of navigation on the novices performance is reversed due to virtual needle guidance by reducing total needle in plane percentage (US guided vs US + Nav + NG guided; p = 0.001 for novices and experts vs novices; p=0.012). Nonetheless, no prominent differences in the visualization aspects between both groups were found.

4. Discussion

Through this study, we have underlined that detailed movement analysis complemented with a dexterity and decision making scoring system makes it possible to quantify the impact of PET-CT-based computer-assisted navigation strategies on a US guided percutaneous biopsy procedure. More specifically, extracting movement components from the recorded needle and ultrasound probe trajectories has allowed us to determine which aspects relate to the decision making and which ones to the dexterity. Furthermore, our findings suggest that mistakes in the decision making process (corrections and retractions; see Figure 6A) provided prominent metrics in the performance analysis. These combined analysis revealed that the impact created by the navigation technologies on the needle placement varied between experts and novices and different features were of importance for different groups.

Our evaluations show that complementing US-guidance with navigation strategies[24-27], based on co-registration of intraprocedural US and preprocedural PET-CT, helps improve movement consistency and fluency for the novices group. This yielded in a dexterity score improvement from Dx_{80} = 20.0 to Dx_{80} = 5.19 (see Figure 5Bii). Navigation reduced the number of corrections (see Figure 6A) and also yields a substantially better decision making score DM_{80} = 12.6 vs DM_{80} = 2.78 (see Figure 6Bii). In contrast, in the expert group the addition of navigation led to a drop in dexterity score, going from Dx_{80} = 2.92 to Dx_{80} = 12.1 (see Figure 5Bi). This suggest that the addition of this extra data decreased temporal features rather than promote consistency. Navigation further increased the number of corrections while maintaining the number of retractions (see Figure 6A), a trend that was also reflected in the worsened decision making score DM_{80} = 0.569 vs DM_{80} = 7.66 (see Figure 6Bi). Combined these finding indicates that the guidance provided by navigation has most value for the inexperienced.[28]

Adding a second feature, in the form of needle guidance[29,30], to complement the navigation process reduced the movement fluency for both groups (see Figure 5A). Interestingly, for the novices the increasing procedural complexity gave a rise in corrections (Figure 6A) and worsened the dexterity and decision making score compared to the above discussed use of navigation, Dx_{80} = 5.19 vs Dx_{80} = 9.73 and DM_{80} = 2.78 vs DM_{80} = 5.90, respectively (see Figure 5Bii and 6Bii). This technology allowed the expert group to score better for both dexterity and decision making when compared to the use of navigation Dx_{80} = 12.1 vs Dx_{80} = 9.33 and DM_{80} = 7.66 vs DM_{80} = 6.38, respectively (see Figure 5Bi and 6Bi). These scores, however, were still inferior to those obtained using US guided only. This suggests that the virtual needle guidance feature can to some degree technological advance but currently negatively influences the experts' performance. In the questionnaires participants pointed out to be distracted by the small misregistrations that the navigation and virtual needle guidance software indicated.

The additional technology when compared to the conventional US guidance had little influence on the US probe movements. However, the observed decrease in: speed, jerkiness, and inversed angular dispersion could indicate in a more efficient and focused localization of biopsy site. This trend is clearly visible through the additional navigation for the novices. This indicates that navigation could be of assistance in the spatial ability training during ultrasonography.[28]

In line with GPS-based route planning in daily life, we expected that navigation and prediction of the ideal route would prove to be very useful tools for needle placement. An assumption that is in line with England J. et al.[31]. Our findings suggest that, despite the technology being CE-marked and available for in human use, the use of navigation technologies in needle guidance is not very intuitive for end-users. Here it must be noted that during the experiments performed, the possibility of a

learning curve was eliminated. Most likely additional training would lead to adequate use of these technologies. A logical next step would thus be to use the analytical metrics defined in this study to monitor progression along the technologies learning curve, ultimately resulting in procedural proficiency.[32-34] Since we were able to directly relate dexterity related features to missteps (see Figure 4), actively improving the dexterity through training could potentially help increasing procedural accuracy. To raise the accuracy of the regression factors in the decision making scoring system we need to increase the sample size. Lastly, the current work is limited to phantom exercises. Future translational efforts should therefore incorporate use in large animal models, human cadavers and or clinical trials.

Entailed movement analysis of an interventional procedure does not only address needs in procedural training[32,35,36], but also open up possibilities with regard to the quantification of the impact that a technology brings.[37] This also opens up the ability to further analyze if/how PET-CT guided interventions can benefit percutaneous biopsy in patients. At the same time, having scoring metrics now also allows us to score the user group specific impact of a technology.

5. Conclusion

Using dedicate movement analysis we were able to quantitatively assess and compare technologies that can be used to guide percutaneous needle placement. This was realized by scoring handling for dexterity, decision making and missteps. Our early preclinical findings underline the potential of value-based scoring strategies, but required further validation in (clinical) follow-up studies.

6. References

1. Valdés Olmos RA, Vidal-Sicart S. Introducing new perspectives in radioguided intervention. Clinical and Translational Imaging 2016;4(5):307-311.
2. El-Haddad G. PET-Based Percutaneous Needle Biopsy. PET Clinics 2016;11(3):333-349.
3. Kobayashi K, Bhargava P, Raja S, Nasseri F, Al-Balas HA, Smith DD, et al. Image-guided Biopsy: What the Interventional Radiologist Needs to Know about PET/CT. RadioGraphics 2012;32(5):1483-1501.
4. Caoili EM, Davenport MS. Role of percutaneous needle biopsy for renal masses. Semin Intervent Radiol 2014;31(1):20-26. (In eng).
5. Gupta S, Madoff DC. Image-Guided Percutaneous Needle Biopsy in Cancer Diagnosis and Staging. Techniques in Vascular and Interventional Radiology 2007;10(2):88-101.
6. Kettritz U. Minimally Invasive Biopsy Methods – Diagnostics or Therapy? Personal Opinion and Review of the Literature. Breast Care 2011;6(2):94-97.
7. Novoa E, Gürtler N, Arnoux A, Kraft M. Role of ultrasound-guided core-needle biopsy in the assessment of head and neck lesions: A meta-analysis and systematic review of the literature. Head & Neck 2012;34(10):1497-1503.
8. Sánchez Y, Anvari A, Samir AE, Arellano RS, Prabhakar AM, Uppot RN. Navigational Guidance and Ablation Planning Tools for Interventional Radiology. Current Problems in Diagnostic Radiology 2017;46(3):225-233.
9. Maybody M, Stevenson C, Solomon SB. Overview of navigation systems in image-guided interventions. Techniques in Vascular and Interventional Radiology 2013;16(3):136-143.
10. Wood BJ, Zhang H, Durrani A, Glossop N, Ranjan S, Lindisch D, et al. Navigation with Electromagnetic Tracking for Interventional Radiology Procedures: A Feasibility Study. Journal of Vascular and Interventional Radiology 2005;16(4):493-505.
11. Kao LS, Thomas EJ. Navigating Towards Improved Surgical Safety Using Aviation-Based Strategies. Journal of Surgical Research 2008;145(2):327-335.

12. Kinahan PE, Fletcher JW. Positron emission tomography-computed tomography standardized uptake values in clinical practice and assessing response to therapy. Seminars in Ultrasound, CT and MRI: Elsevier; 2010:496-505.
13. Kumar V, Nath K, Berman CG, Kim J, Tanvetyanon T, Chiappori AA, et al. Variance of standardized uptake values for FDG-PET/CT greater in clinical practice than under ideal study settings. Clinical nuclear medicine 2013;38(3):175.
14. Hakime A, Deschamps F, De Carvalho EGM, Barah A, Auperin A, De Baere T. Electromagnetic-tracked biopsy under ultrasound guidance: preliminary results. Cardiovascular and interventional radiology 2012;35(4):898-905.
15. Bluemel C, Matthies P, Herrmann K, Povoski SP. 3D scintigraphic imaging and navigation in radioguided surgery: freehand SPECT technology and its clinical applications. Expert Review of Medical Devices 2016;13(4):339-351.
16. Maier-Hein L, Franz A, Meinzer H-P, Wolf I. Comparative assessment of optical tracking systems for soft tissue navigation with fiducial needles. Medical Imaging 2008: Visualization, Image-Guided Procedures, and Modeling: International Society for Optics and Photonics; 2008:69181Z.
17. Estevez I, Christman MC. Analysis of the movement and use of space of animals in confinement: The effect of sampling effort. Applied Animal Behaviour Science 2006;97(2):221-240.
18. Fard MJ, Ameri S, Darin Ellis R, Chinnam RB, Pandya AK, Klein MD. Automated robot-assisted surgical skill evaluation: Predictive analytics approach. The International Journal of Medical Robotics and Computer Assisted Surgery 2018;14(1):e1850.
19. Kearns WD, Fozard JL, Nams VO. Movement Path Tortuosity in Free Ambulation: Relationships to Age and Brain Disease. IEEE Journal of Biomedical and Health Informatics 2017;21(2):539-548.
20. Ghasemloonia A, Maddahi Y, Zareinia K, Lama S, Dort JC, Sutherland GR. Surgical Skill Assessment Using Motion Quality and Smoothness. Journal of Surgical Education 2017;74(2):295-305.
21. Kim SY, Chung HW, Oh TS, Lee J-S. Practical guidelines for ultrasound-guided core needle biopsy of soft-tissue lesions: transformation from beginner to specialist. Korean journal of radiology 2017;18(2):361.
22. Johnson SJ, Hunt CM, Woolnough HM, Crawshaw M, Kilkenny C, Gould DA, et al. Virtual reality, ultrasound-guided liver biopsy simulator: development and performance discrimination. The British Journal of Radiology 2012;85(1013):555-561.
23. Scott DJ. Proficiency-Based Training for Surgical Skills. Seminars in Colon and Rectal Surgery 2008;19(2):72-80.
24. Appelbaum L, Sosna J, Nissenbaum Y, Benshtein A, Goldberg SN. Electromagnetic Navigation System for CT-Guided Biopsy of Small Lesions. American Journal of Roentgenology 2011;196(5):1194-1200.
25. Chehab MA, Brinjikji W, Copelan A, Venkatesan AM. Navigational Tools for Interventional Radiology and Interventional Oncology Applications. Semin Intervent Radiol 2015;32(4):416-427. (In eng).
26. Kagadis GC, Katsanos K, Karnabatidis D, Loudos G, Nikiforidis GC, Hendee WR. Emerging technologies for image guidance and device navigation in interventional radiology. Medical Physics 2012;39(9):5768-5781.
27. Wood BJ, Kruecker J, Abi-Jaoudeh N, Locklin JK, Levy E, Xu S, et al. Navigation systems for ablation. Journal of Vascular and Interventional Radiology 2010;21(8):S257-S263.
28. McVicar J, Niazi AU, Murgatroyd H, Chin KJ, Chan VW. Novice Performance of Ultrasound-Guided Needling Skills: Effect of a Needle Guidance System. Regional Anesthesia & Pain Medicine 2015;40(2):150-153.

29. de Jong TL, van de Berg NJ, Tas L, Moelker A, Dankelman J, van den Dobbelsteen JJ. Needle placement errors: do we need steerable needles in interventional radiology? Med Devices (Auckl) 2018;11:259-265. (In eng).
30. Tielens LKP, Damen RBCC, Lerou JGC, Scheffer G-J, Bruhn J. Ultrasound-guided needle handling using a guidance positioning system in a phantom. Anaesthesia 2014;69(1):24-31.
31. England JR, Fischbeck T, Tchelepi H. The Value of Needle-Guidance Technology in Ultrasound-Guided Percutaneous Procedures Performed by Radiology Residents: A Comparison of Freehand, In-Plane, Fixed-Angle, and Electromagnetic Needle Tracking Techniques. Journal of Ultrasound in Medicine 2019;38(2):399-405.
32. Mirza S, Athreya S. Review of Simulation Training in Interventional Radiology. Academic Radiology 2018;25(4):529-539.
33. Reiley CE, Lin HC, Yuh DD, Hager GD. Review of methods for objective surgical skill evaluation. Surgical Endoscopy 2011;25(2):356-366.
34. Wilcox V, Trus T, Salas N, Martinez J, Dunkin BJ. A Proficiency-Based Skills Training Curriculum for the SAGES Surgical Training For Endoscopic Proficiency (STEP) Program. Journal of Surgical Education 2014;71(3):282-288.
35. Fulton N, Buethe J, Gollamudi J, Robbin M. Simulation-Based Training May Improve Resident Skill in Ultrasound-Guided Biopsy. American Journal of Roentgenology 2016;207(6):1329-1333.
36. Siragusa DA, Cardella JF, Hieb RA, Kaufman JA, Kim HS, Nikolic B, et al. Requirements for training in interventional radiology. J Vasc Interv Radiol 2013;24(11):1609-1612. (In eng).
37. Azargoshasb S, Houwing KHM, Roos PR, Van Leeuwen SI, Boonekamp M, Mazzone E, et al. Optical navigation of a DROP-IN gamma probe as a means to strengthen the connection between robot-assisted and radioguided surgery. Journal of Nuclear Medicine 2021:jnumed.120.2597.
38. Van Oosterom MN, Rietbergen DDD, Welling MM, Van Der Poel HG, Maurer T, Van Leeuwen FWB. Recent advances in nuclear and hybrid detection modalities for image-guided surgery. Expert Review of Medical Devices 2019;16(8):711-734.
39. Hawkes DJ, Barratt D, Blackall JM, Chan C, Edwards PJ, Rhode K, et al. Tissue deformation and shape models in image-guided interventions: a discussion paper. Medical Image Analysis 2005;9(2):163-175.
40. Oliveira-Santos T, Klaeser B, Weitzel T, Krause T, Nolte L-P, Peterhans M, et al. A navigation system for percutaneous needle interventions based on PET/CT images: Design, workflow and error analysis of soft tissue and bone punctures. Computer Aided Surgery 2011;16(5):203-219.
41. van Oosterom MN, Meershoek P, KleinJan GH, Hendricksen K, Navab N, van de Velde CJ, et al. Navigation of fluorescence cameras during soft tissue surgery—is it possible to use a single navigation setup for various open and laparoscopic urological surgery applications? The Journal of urology 2018;199(4):1061-1068.
42. van Oosterom MN, van der Poel HG, Navab N, van de Velde CJH, van Leeuwen FWB. Computer-assisted surgery: virtual- and augmented-reality displays for navigation during urological interventions. Current Opinion in Urology 2018;28(2):205-213.
43. Mani V, Arivazhagan S. Survey of medical image registration. Journal of Biomedical Engineering and Technology 2013;1(2):8-25.
44. Oliveira FPM, Tavares JMRS. Medical image registration: a review. Computer Methods in Biomechanics and Biomedical Engineering 2014;17(2):73-93.
45. Jain S, Kanwal N. Overview on image registration. 2014 International Conference on Medical Imaging, m-Health and Emerging Communication Systems (MedCom): IEEE; 2014:376-381.
46. Krol A, Unlu MZ, Baum KG, Mandel JA, Lee W, Coman IL, et al. MRI/PET nonrigid breast-image registration using skin fiducial markers. Physica Medica 2006;21:39-43.

47. Franz AM, Haidegger T, Birkfellner W, Cleary K, Peters TM, Maier-Hein L. Electromagnetic Tracking in Medicine—A Review of Technology, Validation, and Applications. IEEE Transactions on Medical Imaging 2014;33(8):1702-1725.
48. Nafis C, Jensen V, Beauregard L, Anderson P. Method for estimating dynamic EM tracking accuracy of surgical navigation tools. Medical Imaging 2006: Visualization, Image-Guided Procedures, and Display: International Society for Optics and Photonics; 2006:61410K.
49. Appelbaum L, Mahgerefteh SY, Sosna J, Goldberg SN. Image-guided fusion and navigation: applications in tumor ablation. Techniques in Vascular and Interventional Radiology 2013;16(4):287-295.
50. Lin Q, Yang R, Cai K, Guan P, Xiao W, Wu X. Strategy for accurate liver intervention by an optical tracking system. Biomed Opt Express 2015;6(9):3287-3302.

Appendix A. Phantom Development

To facilitate a dexterity and decision making analysis of additional technology in a conventional US-guided biopsy procedure, a customized abdominal phantom was developed. The decisions taken about the phantom design and criteria are elaborated in this appendix as well as a detailed preparation description and reusing protocol of the phantom.

A.1 Phantom Design Criteria

In the increasingly favored minimal-invasive biopsy, additional technology have been developed to help reach more difficult seated lesion or provide assistance reaching poorly visible lesions. Such complex indications are mainly located in the abdominal region, hence, the design of the phantom was inspired by the abdominal anatomy through including several bone-like structures, e.g. ribs and a spine, and numerous lesions of varying diameters of 1.0, 1.5 and 2.0 cm. The nature of the study, lead us to pursue the following criteria during the development of the phantom;

- The phantom had to be compatible with US, CT, PET and SPECT imaging modalities.
- The materials should be cost-effective, reusable and preservable.
- The materials should provide a familiar feel during the biopsy procedure.
- The design of the lesions should allow for safe injection of radioactive tracer.

The following materials were chosen to meet the aforementioned requirements. For the tissue-like filling material 10% Ballistic Gelatin (Clear Ballistics, Greenville, SC, USA) was used. The spine and ribs were 3D printed with Rigid Resin 4000 (Formlabs, Somerville, MA, USA) and the target lesions were made of an outer layer 3D printed with Elastic resin (Formlabs, Somerville, MA, USA) filled with a mixture of Sodium Polyacrylate: 432784-250g (Sigma-Aldrich, Saint Louis, MO, USA) and Glycerol >99.0%: G5516-100ML (Sigma-Aldrich, Saint Louis, MO, USA).

The final structural design of the customized phantom, shown in Figure A.1, includes six ribs and a spine enclosed between two plexiglass plates. The ribs and spine were 3D printed and the desired shape of the plexiglass are obtained using a milling technique. A platform attached to the top of one of the plexiglass plates containing both an EM active and optical fiducial tracker ensures an exact correlation between the trackers in the imaging data and the phantom.

Figure A.3. Structural design of the customized abdominal phantom, including six ribs, a spine enclosed between two plexiglass plates and a platform containing both an EM active tracker and an optical fiducial tracker.

A.2 Preparation Procedure

Prior to the preparation process, one of the plexiglass plates is removed and the remaining structure is placed within a custom made mold as shown in Figure A.2A. Heating the Ballistic Gelatin to a temperature of 130 °C for a time span of 4 hours allowed for complete homogenous liquification which is subsequently poured in layers into the mold. Between the layers, each of thickness of around two cm, the poured gelatin is cooled back down to room temperature for around one to two hours per layer to completely solidify. Once the surface of the layer is stable enough to endure the weight of the lesions, two to three lesions are randomly placed in between the layers. This process is then repeated (± 5 times) until the entire phantom is filled. Air bubbles degrade the quality of the US images and are therefore reduced by establishing a more constant flow through interrupting the fall by pouring the gel on top of a spatula before entering the mold Figure A.2B. The final result of the phantom is shown in Figure A.2C.

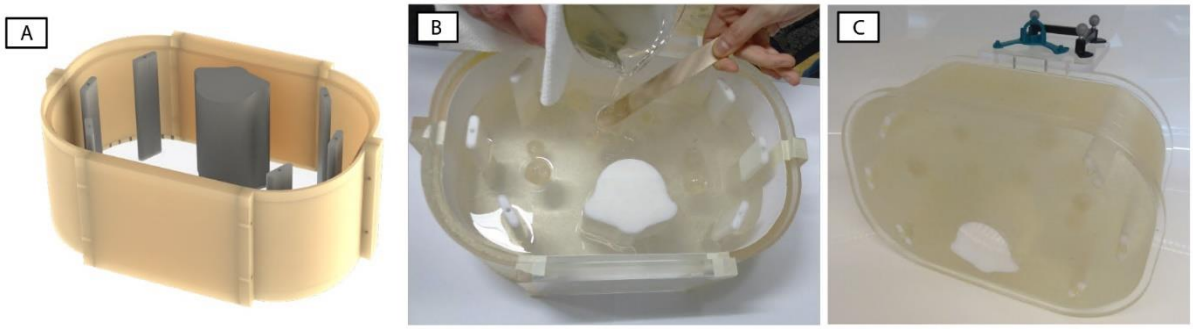

Figure A.4. A) A schematic view of the phantom within the mold. B) depicts the pouring technique used to prepare the phantom with the Ballistic Gelatin and in (C) the resulting customized abdominal phantom is shown.

A.3 Reusing Protocol

Performing a minimal invasive needle biopsy on the phantom, leaves needle tracks within the tissue-like gelatin consisting out of small needle shaped air filled holes within the gelatin. The air is on its turn visible with the US inducing noise in the image and negatively impacts the biopsy procedure by obstructing the target lesions' visibility. Reheating the gelatin within the phantom causes the gel to unify reducing the needle tracks tremendously. However, during this process it is of uttermost importance that the target lesions are kept in the exact same location. Therefore, the gelatin has to be heated on the correct temperature to allow unification while maintaining a certain firmness to ensure the lesions' location. This is achieved by removing the top plexiglass plate and reheating the phantom within early mentioned mold on a temperature of 77 °C for a prolonged duration of 4-8 hours, depending on the amount and depth of the needle tracks. Under these conditions, the gelatin only slightly reshapes, removing majority of the needle tracks while keeping the lesions in place. Afterwards, the phantom is re-established by removing the mold and reattaching the top plexiglass plate after allowing the gelatin to cool down overnight.

Appendix B. Navigation Devices and Tracking Systems

A typical navigated intervention can be divided in 5 important steps; 1) preprocedural imaging, 2) co-registration of images, 3) tracking, 4) intervention, 5) intraprocedural validation which is finalized with confirmation of the postprocedural pathology. In this appendix supplementary information concerning the most commonly used navigational devices and tracking systems to assist complex interventions is provided. Furthermore, the development of customized fiducial-based trackers to establish a navigation workflow of our own, is touched upon in section B.3.

B.1 Image Registration

A navigated intervention starts with the co-registration of preprocedural and intraprocedural images. The preprocedural images often used include CT and less frequent MR images[9] however, can occasionally also be combined with nuclear imaging in which the most important imaging modalities are PET or SPECT. Typically, SPECT imaging is based on low-to-mid energy (<400 keV) gamma emitting radioisotopes (e.g., ^{99m}Tc and ^{111}In), while PET imaging relies on the principle of generation of a high-energy gamma photon pair as a result of the reaction of beta+ emitting radioisotopes (e.g., ^{18}F and ^{68}Ga). The combination of detection of different isotopes with different radiopharmaceuticals, enables targeting of different processes within the human body, e.g. using ^{99m}Tc-nanocolloid based SPECT imaging for Sentinel Lymph Node Biopsy (SLNB) procedures and ^{18}F-FDG for imaging of abnormal metabolic activity with PET imaging.[38] Within a navigational workflow, ultrasonography is the most frequently used modality for intraprocedural imaging. This due to its harmless nature and direct intraprocedural validation. Co-registration of preprocedural images and intraprocedural images facilitates the combination of intraprocedural validation with the established planning roadmap based on preprocedural images. Various registration methods, i.e. landmark-based and fiducial-based registration, allow for such direct translation of these preprocedural images to the real-time position and orientation of the patient during the intervention itself. However, the efficiency of such navigation techniques directly correlates with the adequacy of precise co-registration between the preprocedural images and the patient's position and orientation. Such techniques are susceptible to misalignments caused by patient's internal deformations due to for example the time interval between image acquisition and intervention, different positioning of the patient, breathing motions or even the intervention itself (e.g., pressing on the skin surface or dissection of the tissue). These deformation could result in small or large inaccuracies within the registration, especially for soft-tissue anatomies, causing navigated minimal invasive biopsies to be more challenging.[39-42] In the first option, using landmark-based registration, the accuracy of the registration relies entirely on precise correlation of particular identifiable anatomical landmarks in both the patient scans and intraprocedural coordinate system. This can be done by tipping locations with either a tracked pointer or selecting the same anatomical landmarks on the pre- and intraprocedural images.[43,44] However, using this registration technique is very labor intensive and so in the field of interventional radiology the most common used registration methodology is fiducial-based registration. In this method, fiducial markers are used to recover the transformation between the preprocedural images and the tracking system's coordinate system. By placing fiducial markers on the patient close to the region of interest throughout the acquisition of preprocedural images, the position of these markers are included within the 3D imaging data. Subsequently, the markers are repositioned on the exact same location during the intervention, by for example marking the area of the tracker with indelible ink. The tracking system localizes the fiducials in its coordinate system and correlates this location with the position of the fiducials within the 3D image date. This enables a transformation between the preprocedural 3D image data and its coordinate system to automatically register pre- and intraprocedural images. Each tracking technique requires different kind of fiducials, e.g. an optical tracking system uses reflective spheres as fiducials that are recognizable with a (near) infrared camera while EM based tracking systems uses metal

fiducials causing small distortions within an EM field to localize the position of the fiducials. Co-registration of pre- to intraprocedural images is often referred to as navigation during an intervention procedure.[45,46]

B.2 Device Tracking Techniques

In the next step of a navigation workflow an intervention tool, i.e. a biopsy needle or US probe are in real-time localized within a 3D working data set using different device tracking techniques such as EM-, optical-, robotic-, image-based- and mechanical-tracking. In this study, the first two options are exploited and so the focus here lies on EM and optical tracking.

B.2.1 Electromagnetic Tracking

The fundamentals in EM navigation are based on an EM field generator and multiple field sensors. It extracts 3D spatial information by employing an EM field generator to locate the position of the interventional tool in relation to a patient's anatomy.[10] Magnetic fields with known shapes and geometric properties, determined by the geometry of the emitting coil assembly and the type of current sent through the coil, are used to determine the pose of sensors for measuring magnetic flux. Controlling the dynamic behavior of the reference field allows for both spatial position and orientation encoding relative to this reference field. The employment of special sensors enables actual measurements inside this magnetic field to calculate the spatial information of these sensors which is constructed by measuring the magnetic flux through a specific surface within the sensor. Note that magnetic flux Φ $\left[\mathrm{T} = \frac{\mathrm{kg}}{\mathrm{A}\cdot\mathrm{s}^2}\right]$ is a quantification of the gradient over a certain area S $[\mathrm{m}^2]$ within magnetic field B $\left[\mathrm{Wb} = \frac{\mathrm{kg}\cdot\mathrm{m}^2}{\mathrm{A}\cdot s^2}\right]$ as shown in Equation 3,

$$\Phi = \vec{B} \cdot \vec{S}. \tag{3}$$

And so, for this technique to work, the reference field must be inhomogeneous to provide a correlation between the distance from the source and the magnetic flux. When such sensors are in cooperated within the interventional tools, it is possible to accurately localize its position. On the other hand, the orientational information of the tools are obtained using magnetic dipoles within the sensor.[47] In general, EM tracking systems are able to track multiple sensors, and therefore multiple tools simultaneously with an update frequency of 40-250 Hz[48]. The main advantage of navigation based on EM tracking is the ability to track navigational tools without the requirement of a direct line-of-sight, enabling tracking within a human body. On the other hand, the navigational accuracy of EM based navigation relies on the extraction of spatial information within the generated EM field and is therefore is very sensitive to distortions originating from conducting objects. This makes this type of navigation rather unsuitable in environments with metal based instruments such as in a surgical environment.[49] This study uses an EM tracking system provided by VirtuTRAX (Civco, Kalona, IA), in which both the US probe and the needle tip contain searching sensors enabling co-registration between preprocedural PET-CT and intraprocedural US images and needle guidance respectively. Needle guidance provides assistance by showing the predicted needle path in case of insertion.

B.2.2 Optical Tracking

Optical tracking is based on receiving (near) infrared light emitted or reflected from fiducials attached to the tracked instruments with a (near) infrared camera overlooking the procedural area[16] that continuously captures the changes of these markers positions.[50] The functioning of these systems requires an uninterrupted line-of-sight between fiducial markers and camera, hence, optical systems are only able to track the position of visible part of the tool including the markers. The location of the instrument within the patient has to be estimated by calibrating the location of for example the tip of the needle prior to the start of the procedure. Deflections of the instruments caused by e.g. tissue

density within the patient, are not registered and so, the accuracy of optical tracking depends on the rigidity of the tracked instrument.[9] However, contrary to EM tracking, this technique is not susceptible to distortions caused by metal instruments.[27] Due to the inability to read out raw coordinate data from the EM tracking system, an optical tracking system, Declipse®SPECT Open Surgery (SurgicEye GmbH, Munich, Germany), is used to obtain a read out of the instruments x,y,z-coordinates.

B.3 Customized Fiducial Markers

To establish a combined system of both EM tracking for procedural purposes and optical tracking for data acquisition purposes, optical-based fiducial markers had to be placed on the EM navigated tools. The aim, to track both the US probe and biopsy needle simultaneously, was achieved by designing customized fiducial markers for each tool wherein the reflective spheres attached to each tool formed a different pattern. In order to localize the instrument, the near infrared camera overseeing the procedural area, needs to recognize a minimum of three reflective spheres to be able to calculate the tool's position within the reference frame. Considering the nature of a minimal invasive biopsy procedure, the US probe was expected to experience a larger range of movement than the biopsy needle. Therefore, the US probe contained a tracker with four reflective spheres placed under a 45 degree angle enlarging the tracking possibilities, shown in Figure B.1A. For the biopsy needle, the assumption was made that the range of motion of the needle would not excess the 0 and 90 degree mark. Therefore, the reflective spheres forming a three-point pattern were placed under a 90 degree angle in respect to the needle tip as shown schematically in Figure B.1C. Since the trackers will be used in an EM environment, the holders were 3D printed out of plastic material (Tough 2000, Formlabs, Somerville, MA, USA). In order to calibrate the location of the tip of the US probe scanning area and biopsy needle tip in respect to their optical trackers, customized calibration devices were created, shown in Figure B.1B and B.1D.

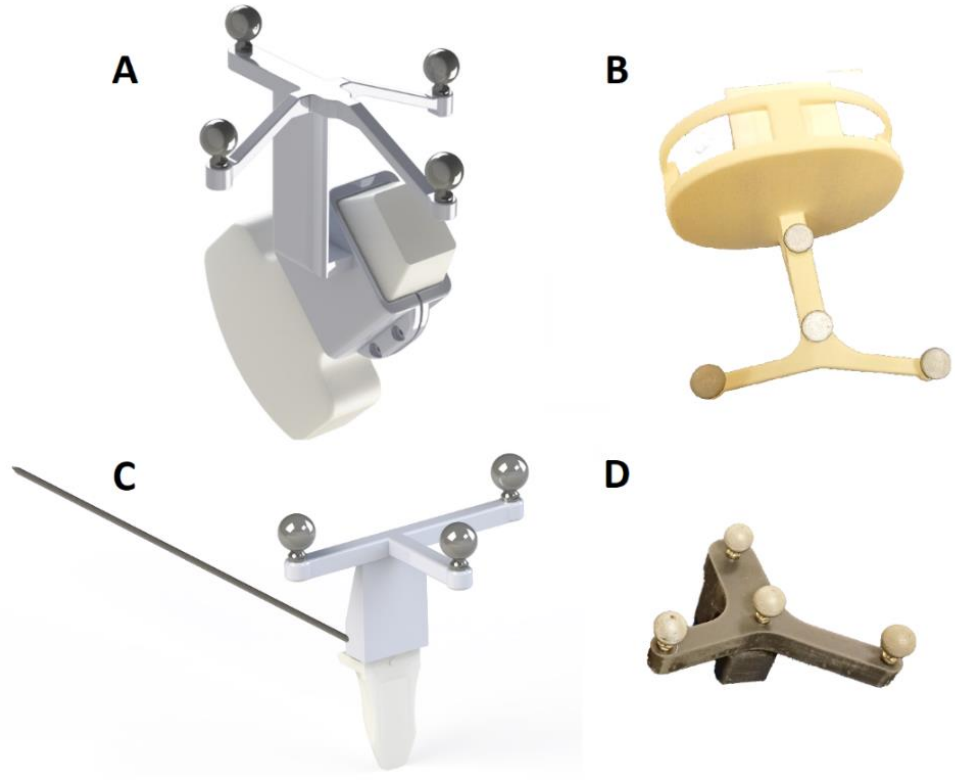

Figure B.1. The customized fiducials placed on the US probe (A) and biopsy needle (C) with its corresponding calibrators (B and D).

Appendix C. Instruction Sheet

In this appendix the instruction sheet given to all the participants prior to the performing the experiment is included.

C.1 General Information

The aim of this experiment is to puncture the metabolic active area of an indicated target located within the phantom (Figure , green arrow) with the tip of the needle (Figure , yellow arrow) in three different situations. Prior to starting the experiment, you are allowed to examine the preprocedural PET-CT images and afterwards you are requested to approach the target. In the first assignment, the biopsy is performed under the guidance of ultrasonography (Figure , red arrow). In the second assignment, navigation will be included wherein the US and pre-procedural PET-CT is automatically co-registered. Here, you are allowed to minimize registration errors by using the landmark registration technique. After co-registration, you are requested to once again puncture the metabolic active part of a new target. In the third and last assignment, you are asked to repeat the procedure when both navigation and needle guidance are provided to you.

Prior to starting the procedure, read the entire step-by-step guide per assignment and perform all steps in one go without pauses.

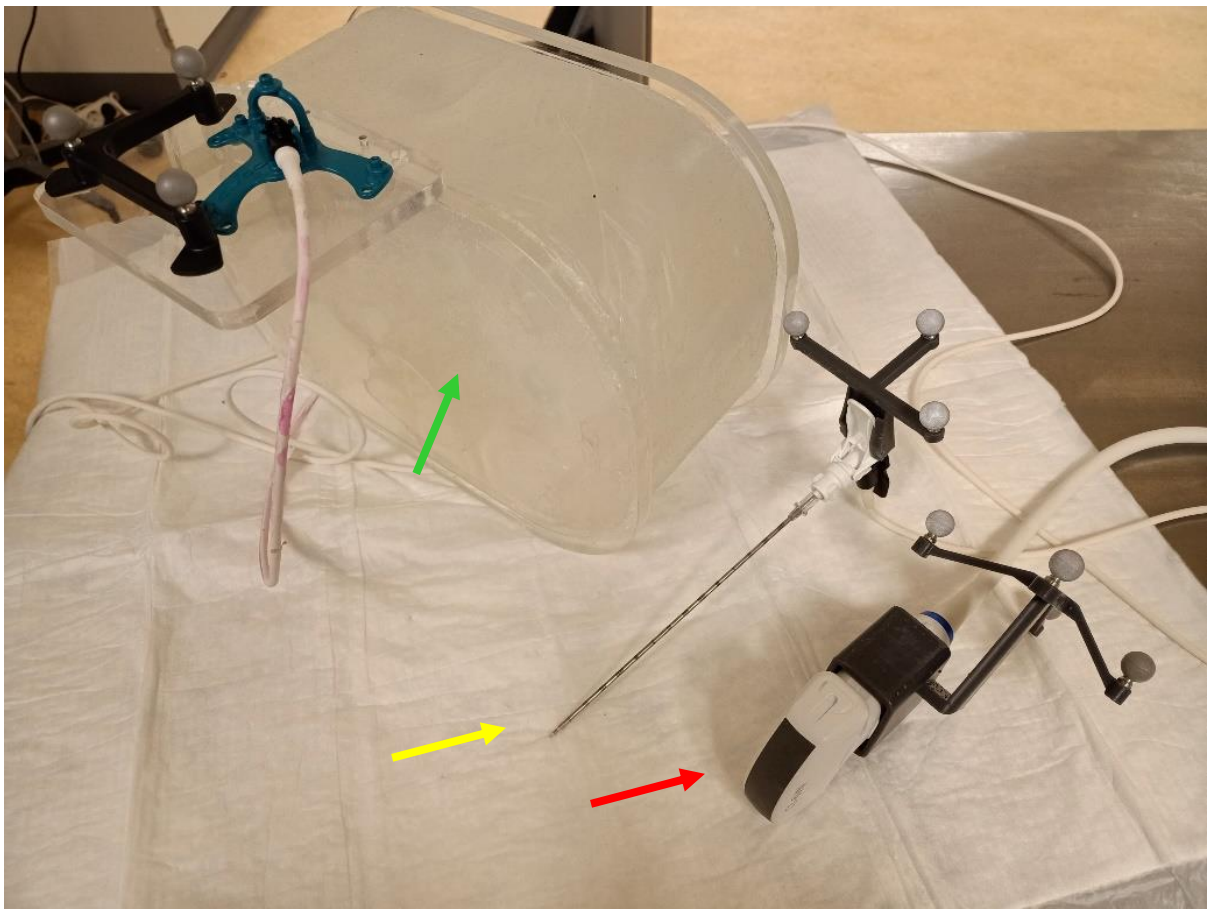

Figure C.1. Set up of the experiments with the phantom (green arrow), the biopsy needle (yellow arrow) and US probe (red arrow).

C.2 Assignment 1 – Step-by-step guide

1. A target lesion is assigned to you and study the pre-procedural images.
2. Take the US probe in your hand while making sure the reflective spheres are faced upwards for tracking purposes, as shown in Figure C.2. *Note:* you will be handling both the needle and the US probe simultaneously, thus give some thought to your hand placement and which hand will be handling the biopsy needle.
3. Locate the target with the US probe keeping it within the beam of the US.
4. Once the target is found, take the biopsy needle in your other hand (make sure the spheres are facing upwards) and determine your insertion point. *Note:* make sure your insertion point results in your needle entering the phantom within your US beam.
5. Insert the needle inside the phantom and aim to puncture the target. *Note:* you can re-enter or adjust your insertion point. The attempt is finished on indication of suspected success by you.
6. Repeat the attempt if the target has not been hit.

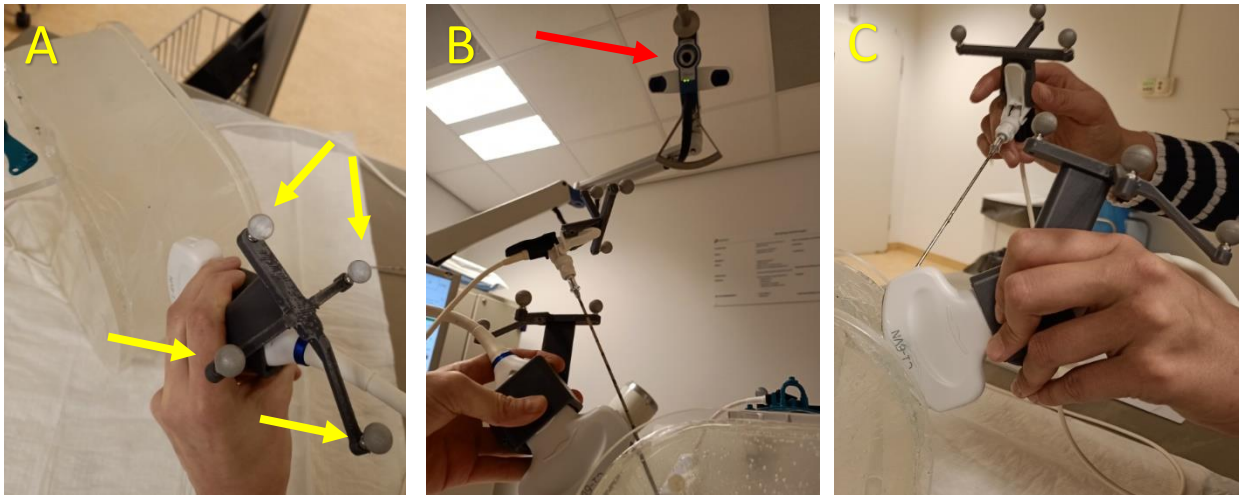

Figure C.2. A) The correct position to hold the probe with the reflective spheres (yellow arrows) facing upwards. B) The reflective spheres should always be in the field of view of the camera (red arrow). C) Shows both hand positions with the reflective spheres facing upwards.

3.3 Assignment 2 – Step-by-step guide

1. A new target is assigned to you and study the pre-procedural images.
2. The navigation will be activated for you, automatically registering the US images with the preprocedural images (Figure C.3).
3. Take the US probe in your hand and make sure the reflective spheres are faced upwards for tracking purposes and determine if you want to make adjustments to the registration to minimize registration errors.
4. If desired, adjust the registration by selecting corresponding points on the US and preprocedural images.
5. Once the registration is correct, start the procedure and find the target with the US keeping it within the beam of the US.
6. Once the target it found, take the biopsy needle in your other hand (make sure the spheres are facing upwards) and determine your insertion point. *Note:* make sure your insertion point results in your needle entering the phantom within your US beam.
7. Insert the needle inside the phantom and aim to puncture the PET-avid target. *Note:* you can re-enter or adjust your insertion point. The attempt is finished on indication of suspected success by you.
8. Repeat the attempt if the target has not been hit.

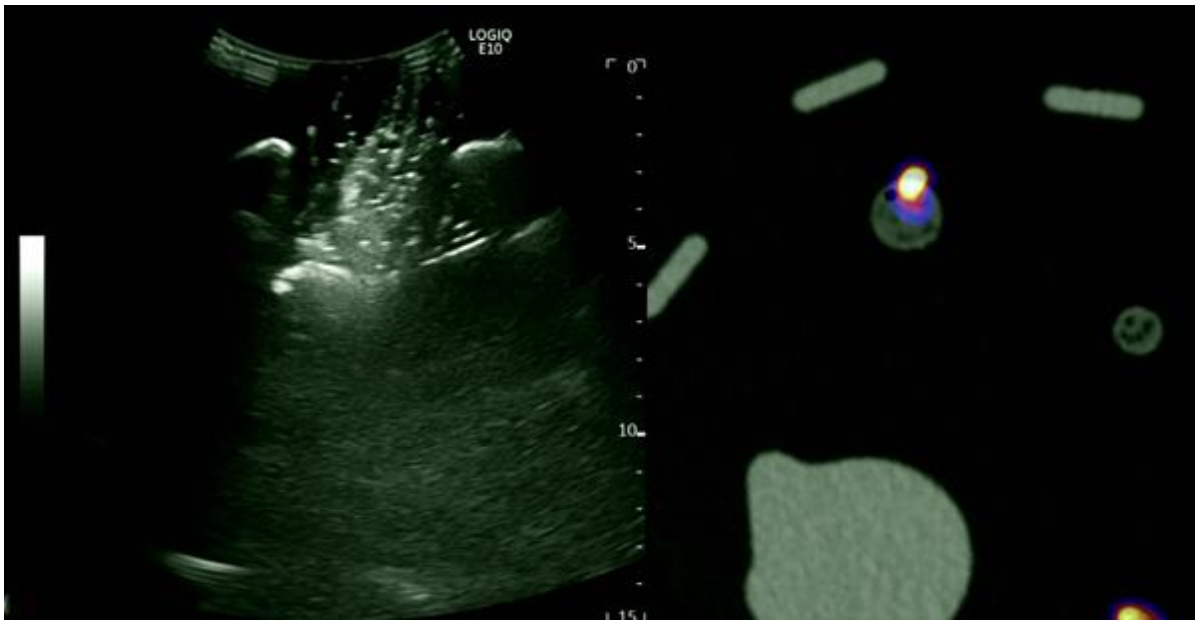

Figure C.3. View on the ultrasound where the preprocedural images are registered to the real-time US.

3.4 Assignment 3 – Step-by-step guide

1. Another target is assigned to you and study the pre-procedural images.
2. The navigation and needle guidance (Figure C.4) will be activated for you, automatically registering the US images with the preprocedural images.
3. Take the US probe in your hand and make sure the reflective spheres are faced upwards for tracking purposes and determine if you want to make adjustments to the registration to minimize registration errors.
4. If desired, adjust the registration by selecting similar points on the US and preprocedural images.
5. Make yourself familiar with the needle guidance by picking up the needle and move it around pretending to enter the phantom.
6. Start the procedure by locating the target with the US.
7. Once the target is found, take the biopsy needle in your other hand (make sure the spheres are facing upwards) and determine your insertion point. *Note:* make sure your insertion point results in your needle entering the phantom within your US beam.
8. Insert the needle inside the phantom and aim to hit the PET-avid target. *Note:* you can re-enter or adjust your insertion point. The attempt is finished on indication of suspected success by you.
9. Repeat the attempt if the target has not been hit.

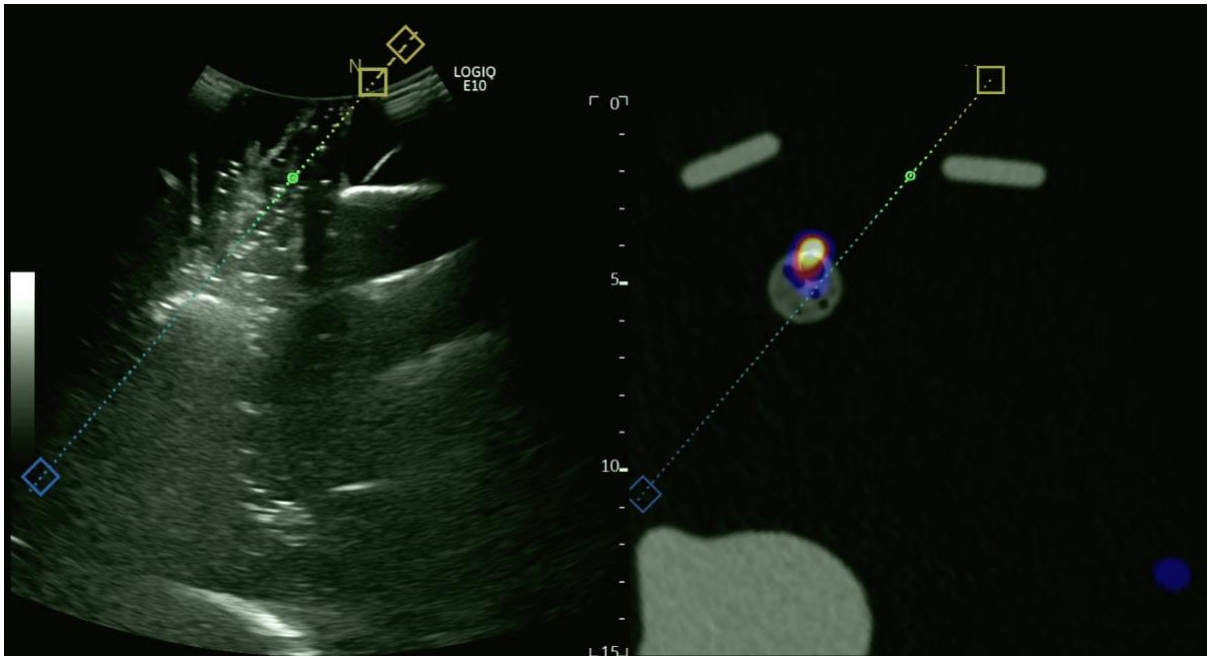

Figure 5. View on the ultrasound where the preprocedural images are registered to the real-time US and the needle guidance showing the predicted path of the needle.

Appendix D. User Experience Questionnaire

In order to obtain insight into the users experience of the additional technology to a conventional biopsy procedure; navigation and needle guidance, and evaluate the usability, participants were asked to fill out a user experience questionnaire (UEQ) for both navigation and needle guidance separately. The usability is divided in three topics; usefulness, ease of use and overall experience and is based on a scoring range from -3 to 3 where 0 represents a neutral opinion. The form provided to the participants after the study can be found in section D.1.

D.1 User Experience Questionnaire Form

Name: _____

Job title:_____

Date: _____

To evaluate the usability and experience of the addition of **navigation** and **needle guidance** to a conventional biopsy procedure, please fill in the two following questionnaires.

The following questions refer to **assignment 2**. How would you describe the usability and experience of the addition of **navigation** to a conventional ultrasonography-guided biopsy procedure.

Table 4.1. Scoring system with a range of -3 to 3 of usability of additional navigation based on 13 individual items.

Usefulness	**-3**	**-2**	**-1**	**0**	**1**	**2**	**3**	
Impractical	☐	☐	☐	☐	☐	☐	☐	Practical
Ineffective	☐	☐	☐	☐	☐	☐	☐	Effective
Inefficient	☐	☐	☐	☐	☐	☐	☐	Efficient
Inferior	☐	☐	☐	☐	☐	☐	☐	Valuable
Conventional	☐	☐	☐	☐	☐	☐	☐	Inventive
Obstructive	☐	☐	☐	☐	☐	☐	☐	Supportive
Ease of use								
Slow	☐	☐	☐	☐	☐	☐	☐	Fast
Complicated	☐	☐	☐	☐	☐	☐	☐	Easy
Confusing	☐	☐	☐	☐	☐	☐	☐	Clear
User Unfriendly	☐	☐	☐	☐	☐	☐	☐	User Friendly
Overall experience								
Difficult to learn	☐	☐	☐	☐	☐	☐	☐	Easy to learn
Boring	☐	☐	☐	☐	☐	☐	☐	Exciting
Annoying	☐	☐	☐	☐	☐	☐	☐	Enjoyable

Additional notes:_____

_____

_____

_____

The following questions refer to **assignment 3**. How would you describe the usability and experience of the addition of **needle guidance** to a navigated ultrasonography-guided biopsy procedure.

Table 4.2. Scoring system with a range of -3 to 3 of usability of additional navigation based on 13 individual items.

Usefulness	**-3**	**-2**	**-1**	**0**	**1**	**2**	**3**	
Impractical	☐	☐	☐	☐	☐	☐	☐	Practical
Ineffective	☐	☐	☐	☐	☐	☐	☐	Effective
Inefficient	☐	☐	☐	☐	☐	☐	☐	Efficient
Inferior	☐	☐	☐	☐	☐	☐	☐	Valuable
Conventional	☐	☐	☐	☐	☐	☐	☐	Inventive
Obstructive	☐	☐	☐	☐	☐	☐	☐	Supportive
Ease of use								
Slow	☐	☐	☐	☐	☐	☐	☐	Fast
Complicated	☐	☐	☐	☐	☐	☐	☐	Easy
Confusing	☐	☐	☐	☐	☐	☐	☐	Clear
User Unfriendly	☐	☐	☐	☐	☐	☐	☐	User Friendly
Overall experience								
Difficult to learn	☐	☐	☐	☐	☐	☐	☐	Easy to learn
Boring	☐	☐	☐	☐	☐	☐	☐	Exciting
Annoying	☐	☐	☐	☐	☐	☐	☐	Enjoyable

Additional notes:_____

_____

_____

_____

D.2 Evaluation of the Users Experience

A total of 15 participants filled out the UEQ form, evaluating the usability of additional navigation and needle guidance based on 13 items, each item subdivided in one of the following scales; attractiveness (purple), perspicuity (gray), efficiency (blue), dependability (cyan), stimulation (red) and novelty (orange). The analysis of the UEQ is based on each individual component, which is then followed by the general comments on the extra technology given by the participants are given.

D.2.1 Usability of Additional Navigation

The overall results based on the mean value per item are shown in Figure D.1, wherein in general each item was graded positively with a score range between 0 and 2 indicating a positive usability towards additional navigation. Interestingly, in the distribution of the answers per item, shown in Figure D.2, only a small percentage of the participants grades the additional navigation negatively.

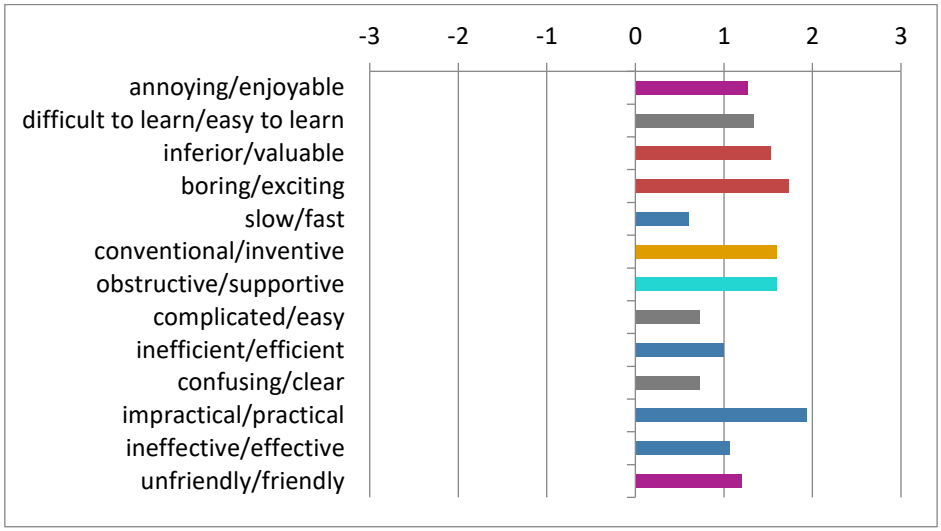

Figure D.1. The mean evaluation value of each item for additional navigation based on a scoring range of -3 to 3 wherein 0 represents neutral and the colors indicate the subdivision scale of each item; attractiveness (purple), perspicuity (gray), efficiency (blue), dependability (cyan), stimulation (ref) and novelty (orange).

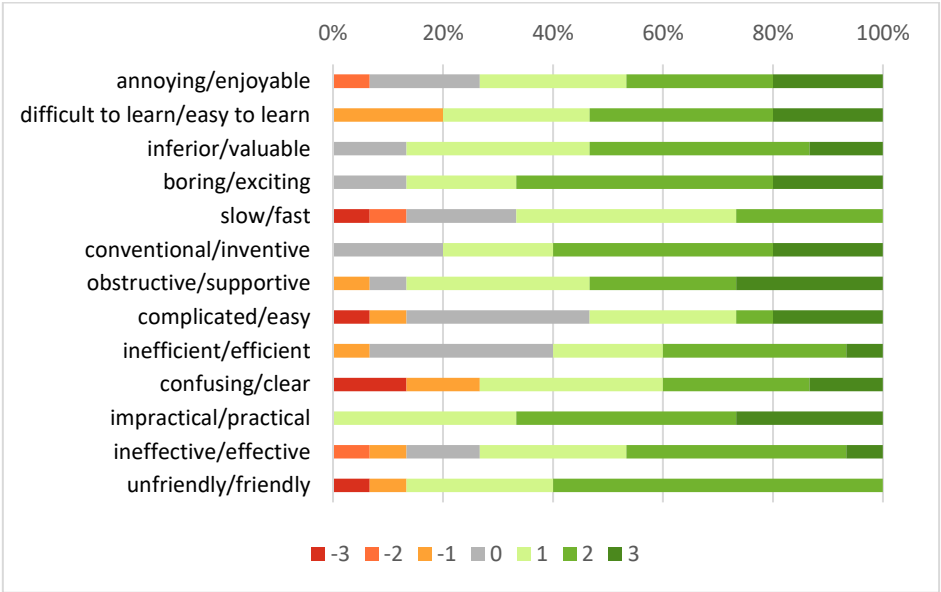

Figure D.2. The distribution in percentage of the answers per item based on the additional navigation evaluation given by the participants.

In general majority of the novices stated that the additional navigation helps to obtain a clear overview and is most beneficial during the orientation process. On the other hand, the experts mainly thought that during simple procedures the navigation is of little value, but finds its significant use in more complex indications. However, the set-up and co-registration of the navigation is labor-intensive and so the active tracker was considered to be a must. Nonetheless, both groups had the opinion that the misregistration between the preprocedural and US images had an obstructive effect on the procedure.

D.2.2 Usability of Additional Needle Guidance

Overall the results, shown in Figure D.3, indicate a favorable evaluation towards the usability of needle guidance based on the mean value per item. Each item was graded within a score range between 1 and 2 implying the usefulness of the additional technology. The low variety within the distribution of the answers per item, shown in Figure D.4, suggest a nearly unanimous and positive opinion towards needle guidance.

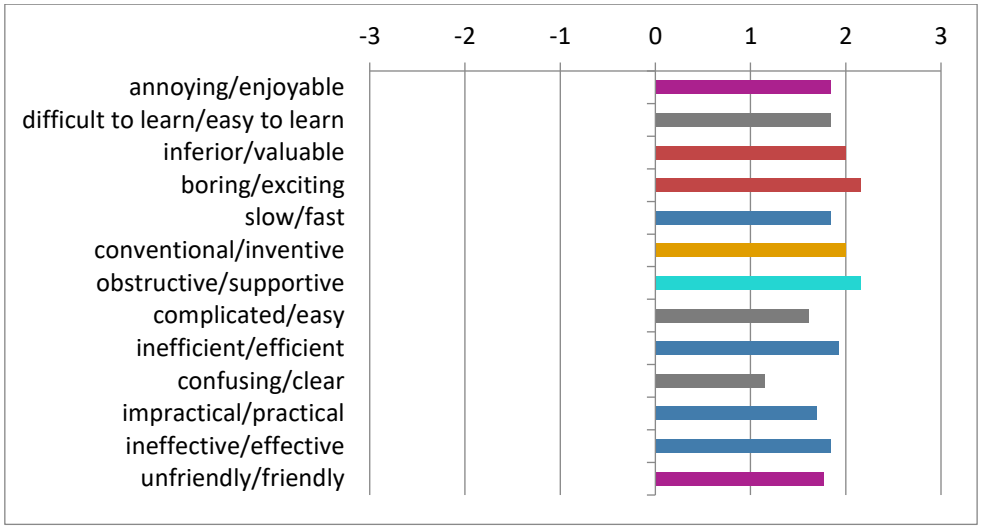

Figure D.3. The mean evaluation value of each item for additional needle guidance based on a scoring range of -3 to 3 wherein 0 represents neutral and the colors indicate the subdivision scale of each item; attractiveness (purple), perspicuity (gray), efficiency (blue),

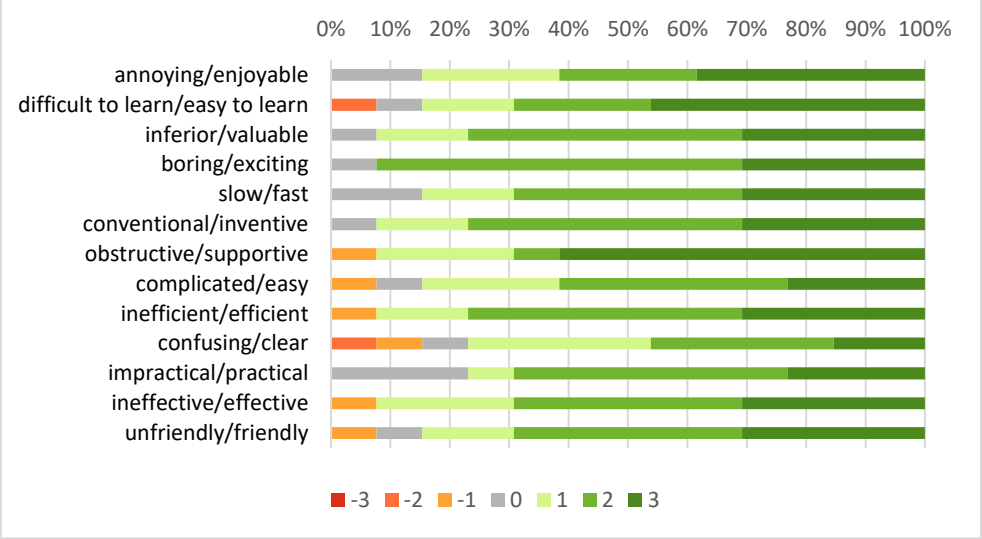

Figure D.4. The distribution in percentage of the answers per item based on the additional needle guidance evaluation given by the participants.

The personal opinion of the participants are in line with the results of the questionnaire. Overall the participants of both groups mentioned the potential of needle guidance and considered it to be most beneficial in deeper seated, poorly visible lesions. However, the amount of information given, such as various different colors and symbols, are judged to be complicated making the technology rather complex and difficult to use. Furthermore, some participants, mainly experts, believed the additional line on the display to be obstructive by altering the attentional focus towards the needle guidance line rather than the real needle on the US-images. Nonetheless, the participants recognized that with training, the efficiency of the technology could increase tremendously.

Appendix E. Trajectory Analysis

In order to analyze the dexterity and decision making of the biopsy procedures and evaluate the role of the different technology aspects of the introduced navigational strategies, the different characteristics of the 3D paths traveled by the US probe and needle over time have to be taken into account. For instance, the motion of the needle can be described through its pathlength but also other features such as its velocity, acceleration, jerkiness and straightness. These characteristics can be transformed into quantitative metrics by applying a kinematic analysis based on a theory successfully used for quantification of robotic surgical movements.[18] The instruments are optically tracked and the obtained 3D coordinate data is firstly preprocessed using MATLAB® (the Mathworks, Inc.) which consisted of applying a nearest neighbor interpolation to fill out the gaps within the trajectories when the instrument was out of the field of view of the tracking camera. In this study, the dexterity is analyzed according to total pathlength, completion time, straightness index and the temporal features such as speed, acceleration, jerkiness, angular dispersion and curvature of both instruments. The decision making process was quantified by extracting the number of corrections and retractions, appearing within the needle trajectory.

Total pathlength: is defined as the total distance the instrument (needle or US probe) traveled over time. The total pathlength s $[\mathrm{mm}]$ is extracted from the data by a summation over all the lengths n between each of data points.

$$s = \sum_{i=1}^{n} dis(p_i, p_{i-1}). \tag{4}$$

Completion time: is based on the duration time of which the instrument is tracked. The camera records the instruments' position with a recording rate of 21 Hz and so calculating the total amount of data points and dividing this by the recording rate allows for completion time determination.

Speed: is the scalar quantity v $[\mathrm{mm} \cdot \mathrm{s}^{-1}]$ described through the rate at which an objects covers a distance. It can be extracted from the data by defining the rate of change in position between data points p_i, p_{i-1};

$$v = \frac{dis(p_i, p_{i-1})}{\Delta t_i}. \tag{5}$$

Here the distance between the data points is described as the Euclidean distance between point p_i and point p_{i-1}. In this study the data points are recorded with a constant frequency of 21 Hz, thus Δt_i is equal to $1/21$ s. Finally, for each participant the median value of the speed determined over the entire trajectory is calculated.

Acceleration: is defined as the second time derivative of position; a $[\mathrm{mm} \cdot s^{-2}]$, which represents the change in speed in between data points. Therefore the acceleration is calculated by taking the derivative of the speed between each data point;

$$a = \frac{\Delta dis(p_i, p_{i-1})}{{\Delta t_i}^2}. \tag{6}$$

Subsequently, the acceleration is normalized and the median value of each trajectory is calculated to describe the acceleration of the track.

Jerkiness: similar as for the acceleration, the jerkiness is described by the third time derivative of its position. Hence, taking the derivative of the acceleration results in the jerkiness J $[\mathrm{mm} \cdot \mathrm{s}^{-3}]$;

$$J = \frac{\Delta^2 dis(p_i, p_{i-1})}{{\Delta t_i}^3}. \tag{7}$$

The motion smoothness of which the instruments moved is finally described by the median value of the jerkiness.

Straightness Index: quantifies the fluctuations of which the instruments deviates from the ideal straight path. The straightness index ST can be described as the ratio between the displacement of two points and the total pathlength[17,19];

$$ST = \frac{dis(p_i, p_{i-1})}{\sum_{i=1}^{n} dis(p_i, p_{i-1})}. \tag{8}$$

Angular Dispersion: describes the number of turning angles diverging from the main instrument's movement angle and thereby quantifies the amount of where the movement pattern switches from linear to circular and vice versa. The angular dispersion AD is calculated as follows;

$$AD = \frac{1}{\theta_i}\sqrt{C^2 + S^2}. \tag{9}$$

Here, θ_i represents the turning angle at each point i, and θ_i, C and S in $[\mathrm{rad}]$ are defined as;

$$\theta_i = \cos^{-1}\left(\frac{\vec{\boldsymbol{U}} \cdot \vec{\boldsymbol{V}}}{\|\vec{\boldsymbol{U}}\| \cdot \|\vec{\boldsymbol{V}}\|}\right), \tag{10}$$

With $\vec{\boldsymbol{U}} = (p_i, p_{i-1})$ and $\vec{\boldsymbol{V}} = (p_{i+1}, p_i)$,

$$C = \sum_{i=1}^{n-1} \cos(\theta_i) \tag{11}$$

$$S = \sum_{i=1}^{n-1} \sin(\theta_i). \tag{12}$$

Curvature: is another measure of the straightness of a path by describing the angle consistency within the trajectory of the instrument. The curvature κ is calculated with the following formula;

$$\kappa = \frac{1}{R_i}. \tag{13}$$

Here R_i depicts radius of the circumcenter based on three data points (p_{i+1}, p_i, p_{i-1}) and can be calculated by taking the length between each the data points; $a = dis(p_i, p_{i-1})$, $b = dis(p_{i+1}, p_i)$ and $c = dis(p_{i+1}, p_{i-1})$,

$$\boldsymbol{R_i} = \frac{\boldsymbol{abc}}{\sqrt{(\boldsymbol{a}+\boldsymbol{b}+\boldsymbol{c})(\boldsymbol{b}+\boldsymbol{c}-\boldsymbol{a})(\boldsymbol{a}+\boldsymbol{b}-\boldsymbol{c})}}. \tag{14}$$

Corrections and retractions: are based on the directional change in the z-direction. The number of corrections and retractions are extracted from the data by defining the directional change between each point; either up or down. Establishing segments within the trajectory wherein the directional change between the data points is equal allows a classification based on the length of the segment l $[\mathrm{mm}]$; corrections ($10 \leq l < 50$ mm), retractions ($l \geq 50$ mm) or small noise within the trajectory ($l < 10$ mm).

Appendix F. In Depth Exploration of the Results

F.1 Determination of Decision Making Regression Factors

The number of extremes in jerkiness ($\#J_{extr}$), retractions (R), corrections (C) and the e powered logarithmic straightness index ($e^{-\log(ST)}$) are all dependent on the total pathlength. To investigate the precision of the dependency, each feature is plotted against the total pathlength of the experts, normalized with a min-max normalization. The resulting regressions of the number of extremes in jerkiness, retractions, corrections and the e powered logarithmic straightness index are equal to 1.684, 3.322, 2.125 and 2.057 respectively with relative R^2 values equal to 0.88, 0.85, 0.60 and 0.67. It should be noted that these relations are determined over a dataset n=20. Enlarging the dataset will strengthened this relation in future research.

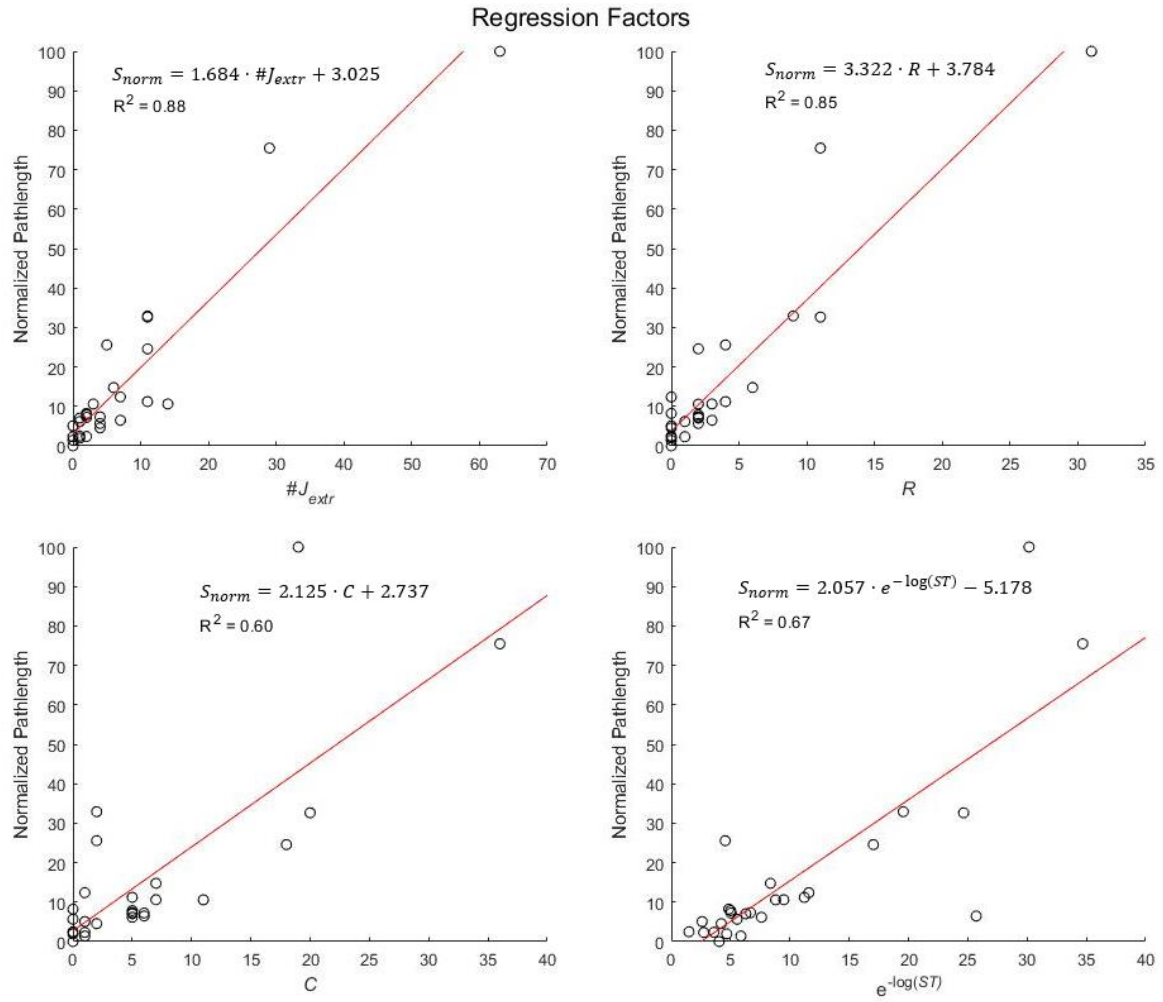

Figure F.1. The linear correlations between the number of extremes in jerkiness ($\#J_{extr}$), retractions (R), corrections (C) and the e powered logarithmic straightness index ($e^{-log\ (ST)}$) and the total pathlength of the experts, normalized with a min-max normalization.

F.2 In Depth Exploration of Movement Features

To provide more in depth information towards the spatial movements of both user groups (gray – experts, white – novices), the median, 25-75 percentiles and extreme ranges of the movement features; speed, acceleration, jerkiness, inversed straightness index, inversed angular dispersion and curvature are depicted in boxplots during the US guided, US + Nav guided and US+ Nav + NG guided biopsies for both the needle (Figure F.2) and US probe (Figure F.3).

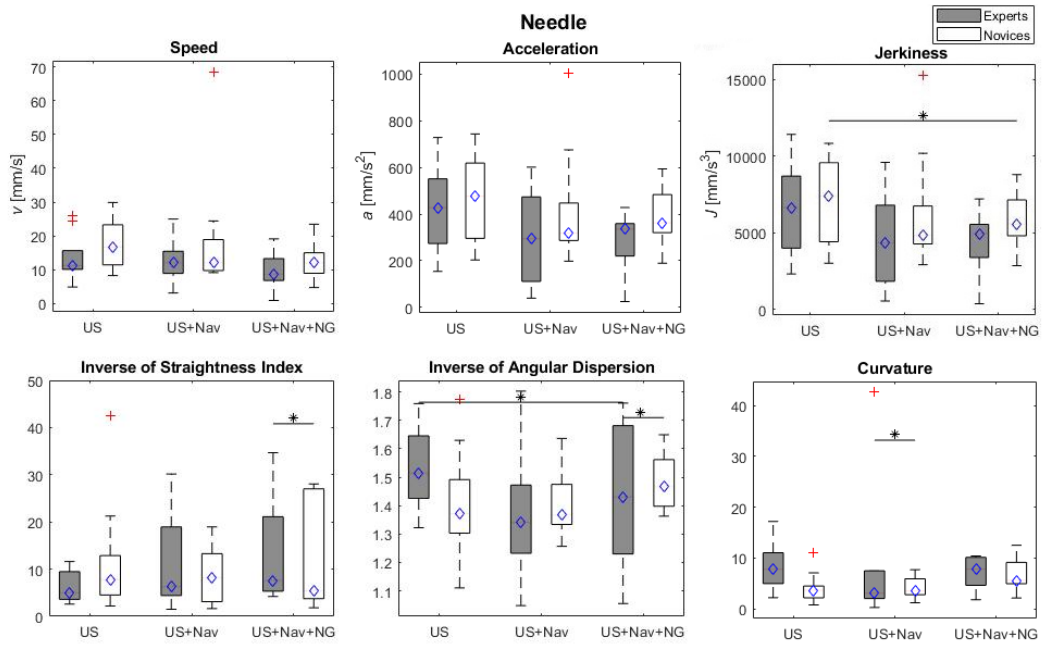

*Figure F.2. The median, 25-75 percentiles and extreme ranges of the movement of the biopsy needle during US guided, US + Nav guided and US+ Nav + NG guided biopsies for the experts (gray) and novices (white). The significance is indicates by *; p<0.05 and **; p<0.01.*

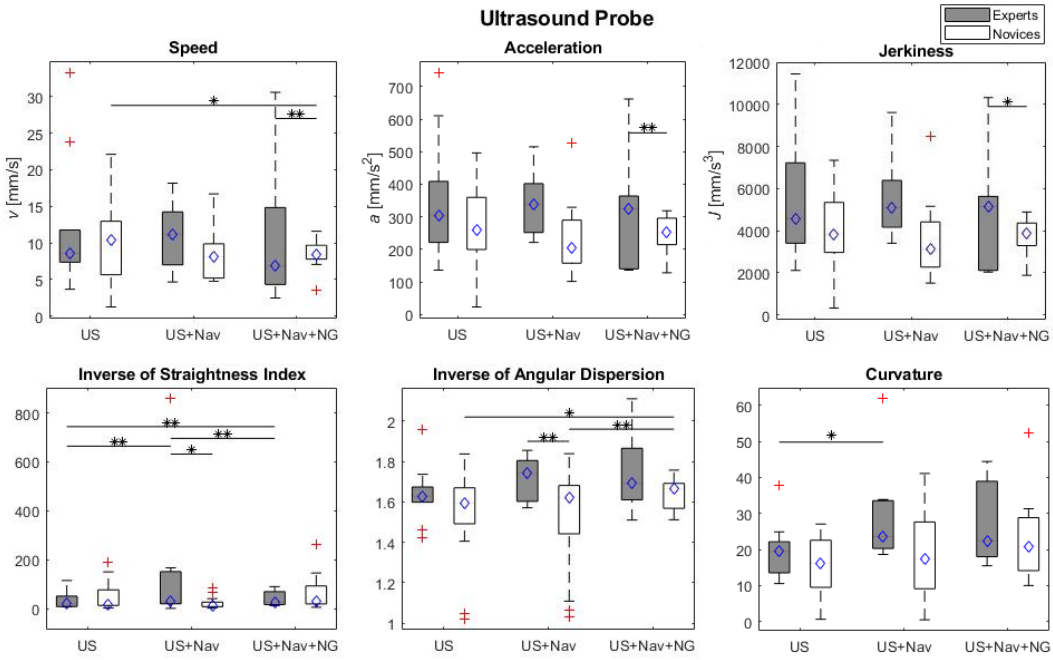

*Figure F.3. The median, 25-75 percentiles and extreme ranges of the movement features of the US probe during US guided, US + Nav guided and US+ Nav + NG guided biopsies for the experts (gray) and novices (white). The significance is indicates by *; p<0.05 and **; p<0.01.*

An overview of the movement features extracted from the US probe trajectories during US guided (red), Us + Nav guided (blue) and US + Nav + NG guided (green) biopsies of both experts (gray) and novices (white) is given in Figure F.4.

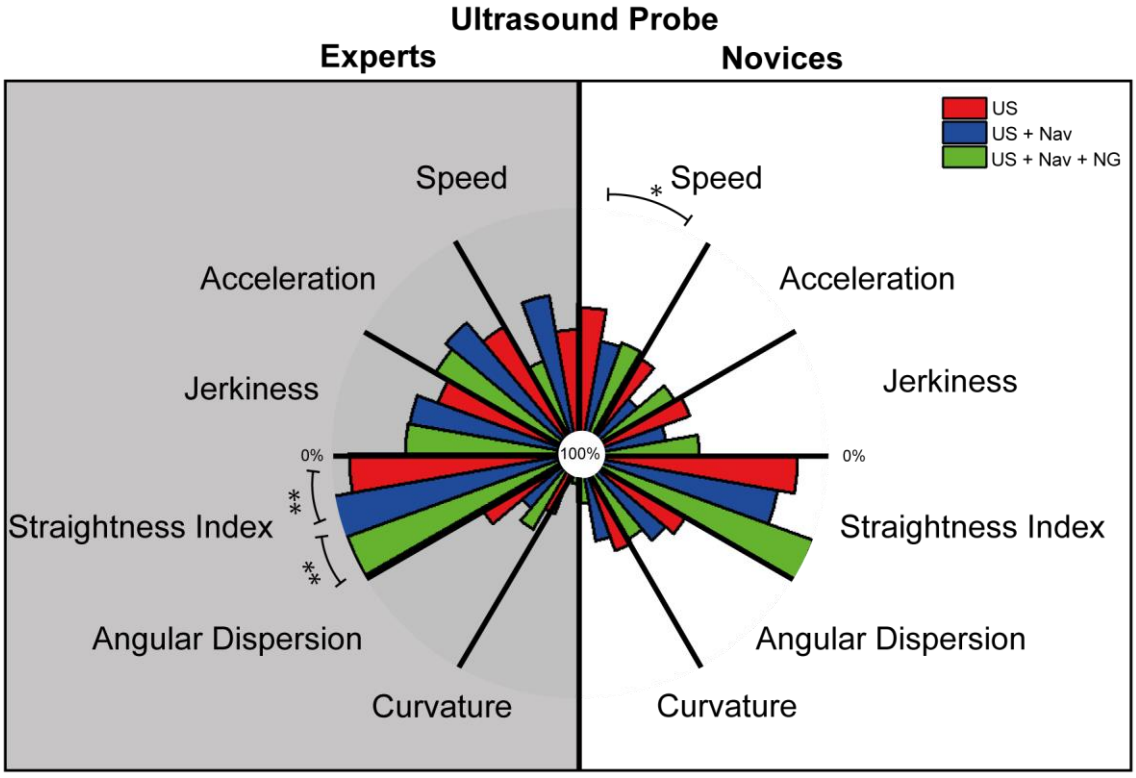

*Figure F.4. Movement feature overview of the US probe during US guided (red), Us + Nav guided (blue) and US + Nav + NG guided (green) biopsies of both experts (gray) and novices (white). The technology comparison significance is indicated with *; p<0.05 and **; p<0.01.*

F.3 Determination of the Group Specific Scores of the Dexterity and Decision Making

In order to evaluate the impact of the additional computer-assisted navigation strategies on the dexterity and decision making during a US-guided biopsy, both user groups, experts (gray) and novices (white), are scored according to the median of the regression line. This is achieved by performing a min-max normalization on the total pathlength of the specific data group in question and plot the result as a function of the corresponding dexterity index and decision making index. The index value that corresponds with a pathlength of 20% in that certain group is defined as the Dx_{80} and DM_{80} scores and is the considered to be the overall group proficiency score based on surgical training programs[23] to compare the different technologies; US guided biopsy, US + Nav guided biopsy and US + Nav + NG guided biopsy. The dexterity index and decision making index per group for these as well as the total data set are shown in Figure F.3 and Figure F.4 respectively.

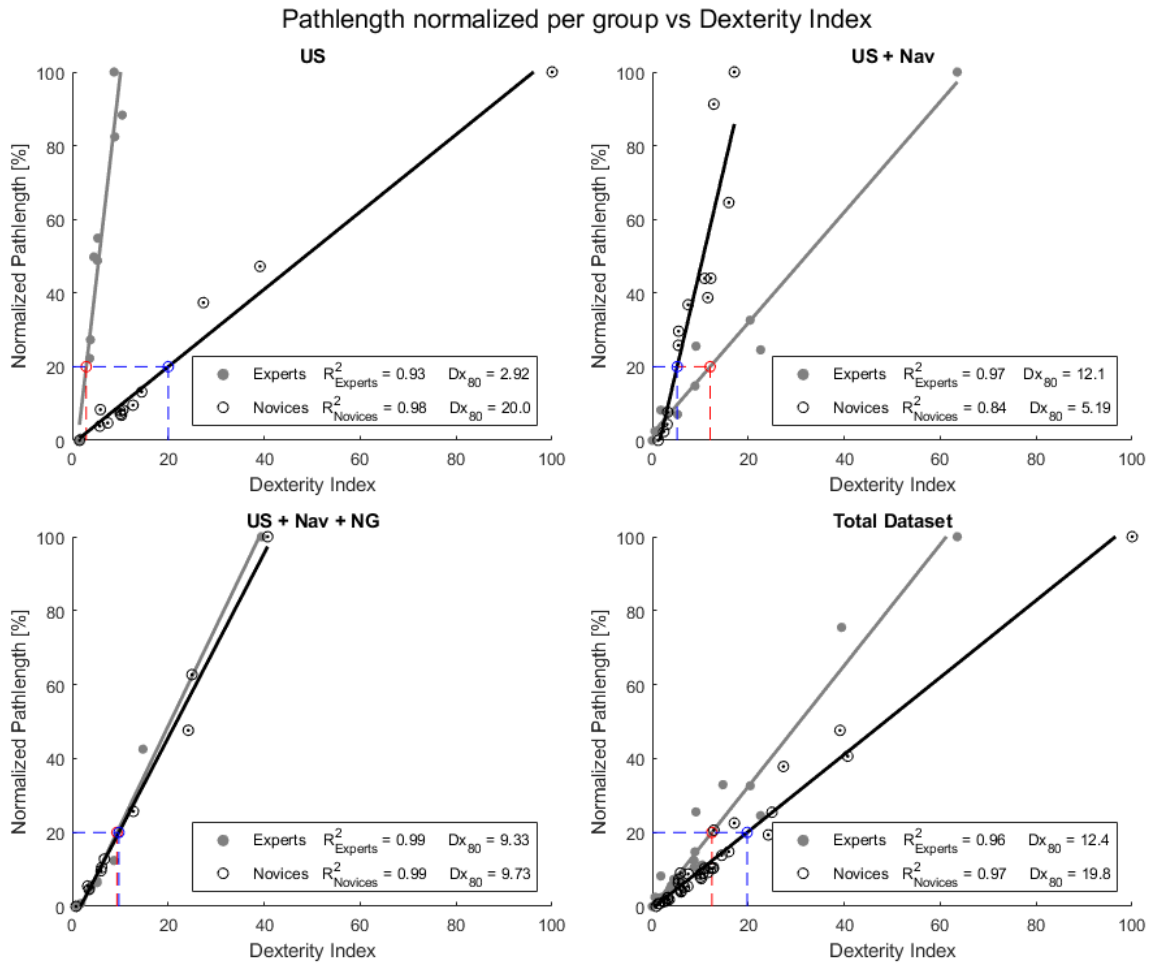

Figure F.5. The dexterity index based on each user group, experts (gray) and novices (white), separately determined for US guided biopsy, US + Nav guided biopsy and US + Nav + NG guided biopsy as well as the total data set. The index value that corresponds with a pathlength of 80% in that certain group is defined as the Dx_{80} score.

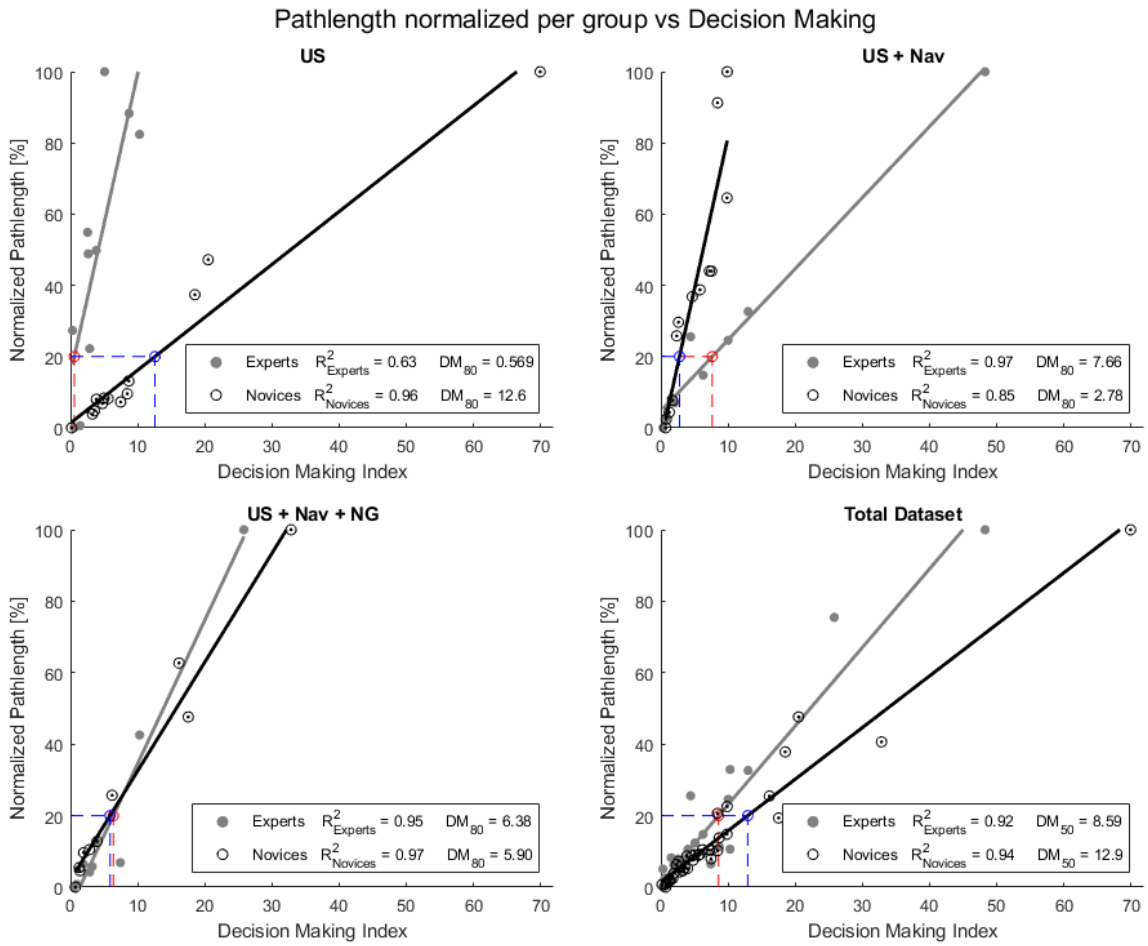

Figure F.6. The decision making index based on each user group, experts (gray) and novices (white), separately determined for US guided biopsy, US + Nav guided biopsy and US + Nav + NG guided biopsy as well as the total data set. The index value that corresponds with a pathlength of 80% in that certain group is defined as the DM_{80} score.

F.4 In Depth Missteps and Decision Making Exploration

More in depth information on the missteps occurring within the needle path for all technologies; US guided, US + Nav guided and US + Nav + NG guided biopsy is for both user groups (experts – gray and novices- white) is given in Figure F.7.

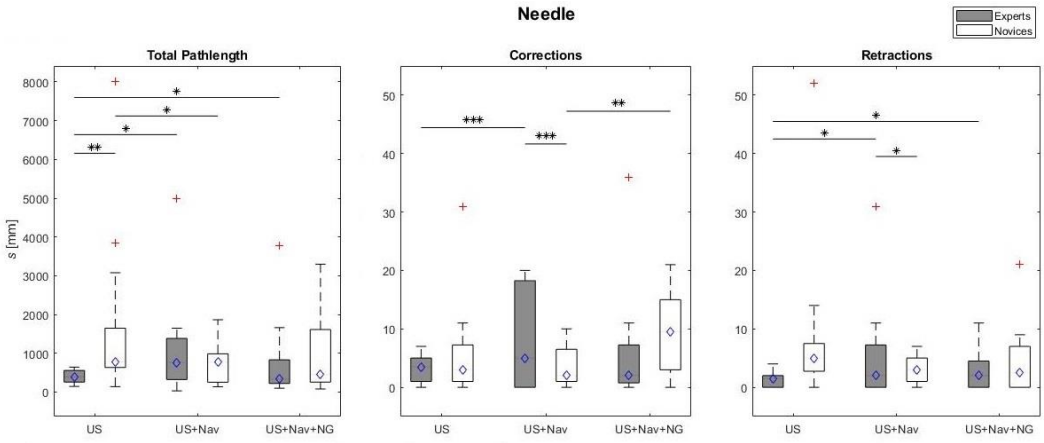

Figure F.7. Boxplots of the total pathlength of the needle trajectory and the corrections and retractions occurring within the needle path for experts (gray) and novices (white) for US guided, US + Nav guided and US + Nav + NG guided biopsy.

An extensive overview of the video analysis; calculation of target in view percentages, needle tip visualization percentages and total needle in plane visualization percentages, performed on the US images for all three exercises performed by both experts (gray) and novices (white) is depicted in boxplots in Figure F.8 and an overviewing comparison of the total US performance during US (red), US + Nav (blue) and US + Nav + NG (green) guided biopsy for both user groups is given in Figure F.9.

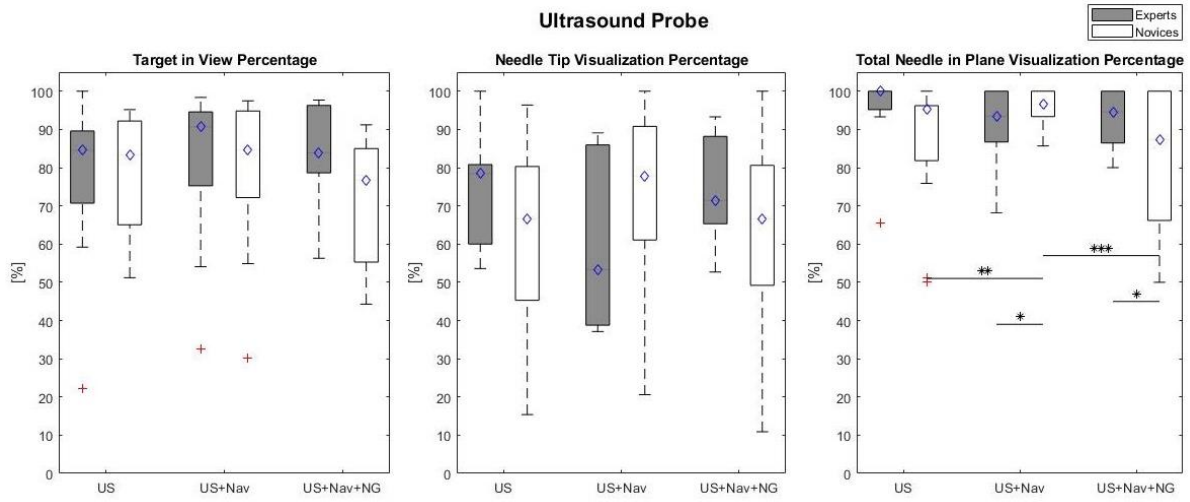

Figure F.8. The target in view, needle tip visualization and total needle in plane visualization percentages extracted from during US, US + Nav and US + Nav + NG guided biopsy for both experts (gray) and novices (white).

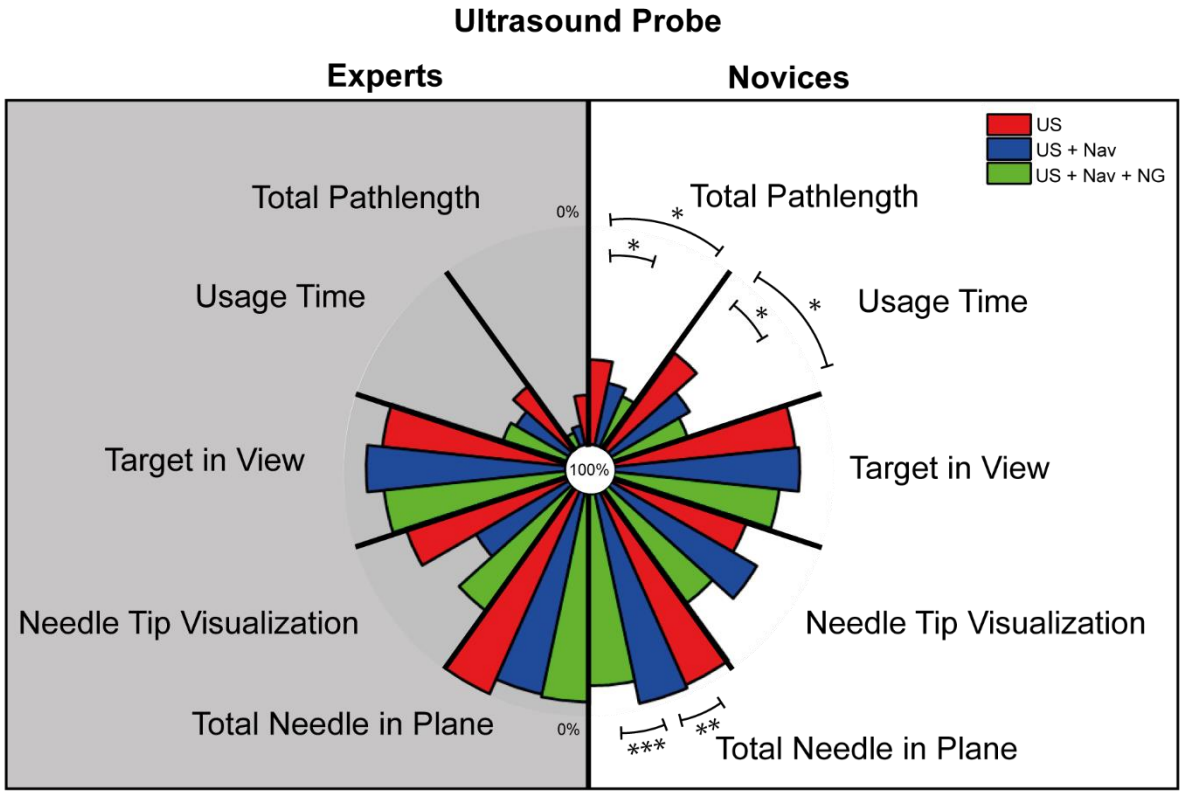

*Figure F.9. An extensive overview of the US performance of both experts (gray) and novices (white) during US (red), US + Nav (blue) and US + Nav + NG (green) guided biopsy. The significance within the comparison is indicated with *; p<0.05, **; p<0.01 and ***; p<0.001.*